Journal of Organometallic Chemistry 1040 (2025) 123829

Contents lists available at ScienceDirect

Journal of Organometallic Chemistry

journal homepage: www.elsevier.com/locate/jorganchem

Chiral Ferrocenylphosphine-amino acid Ligands: Synthesis, characterization, electrochemistry, and coordination to ruthenium (II) complexes

Andrés Terán [a,b], Loreto Hernández [c], Andrés Vega [d], Diego Sierra [a,*]

[a] Laboratorio de Química Organometálica y Catálisis, Instituto de Química y Bioquímica, Facultad de Ciencias, Universidad de Valparaíso, Av. Gran Bretaña 1111, Valparaíso, Chile
[b] Departamento de Química, Universidad Técnica Federico Santa María, Avenida España 1680, Valparaíso, Chile
[c] Laboratorio de Electroquímica, Instituto de Química y Bioquímica, Facultad de Ciencias, Universidad de Valparaíso, Av. Gran Bretaña 1111, Valparaíso, Chile
[d] Departamento de Ciencias Químicas, Facultad de Ciencias Exactas, Universidad Andrés Bello, Av. República 498, Santiago de Chile, Chile

ARTICLE INFO

Keywords:
Ferrocenylphosphines
Amino acids
Electrochemistry
Ruthenium
Bimetallic complexes

ABSTRACT

The synthesis of four ferrocenylphosphine-amino acid ligands, (*S*)-(η^5-C_5H_4-PR_2)Fe(η^5-C_5H_4-AA) [*R*= Ph, AA= *l*-Glu(OMe)$_2$: **5a'**; *R*= Cy, AA= *l*-Glu(OMe)$_2$: **5b'**; *R*= Ph, AA= *l*-Pro(OMe): **5a''**; *R*= Cy, AA= *l*-Pro(OMe): **5b''**] through a new synthetic method is presented along with two solid-state X-ray crystal structures of the corresponding phosphine selenides **5a''^{Se}** and **5b''^{Se}**. Electronic and basicity properties of the ligands were evaluated through the synthesis of the corresponding phosphine selenides **5a'^{Se}** – **5b''^{Se}**. Coordination capabilities of the ferrocenylphosphine-amino acid ligands with the p-cymene ruthenium dichloride dimer was evaluated, affording four neutral complexes, $RuCl_2(\eta^6$-$C_{10}H_{14})\{PR_2$-$[(\eta^5$-$C_5H_4)Fe(\eta^5$-C_5H_4-AA)]\}$ [*R*= Ph, AA= *l*-Glu(OMe)$_2$: **6a'**; *R*= Cy, AA= *l*-Glu(OMe)$_2$: **6b'**; *R*= Ph, AA= *l*-Pro(OMe): **6a''**; *R*= Cy, AA= *l*-Pro(OMe): **6b''**] and three cationic complexes $\langle RuCl(NCMe)(\eta^6$-$C_{10}H_{14})\{PR_2$-$[(\eta^5$-$C_5H_4)Fe(\eta^5$-$C_5H_4$-AA)]\}$\rangle SbF_6$ [*R*= Ph, AA= *l*-Glu(OMe)$_2$: **7a'**; *R*= Ph, AA= *l*-Pro(OMe): **7a''**; *R*= Cy, AA= *l*-Pro(OMe): **7b''**]. All new ligands and complexes were fully characterized by NMR spectroscopy, electrospray ionization mass spectrometry and their electrochemical properties were measured by cyclic voltammetry at a platinum disk electrode.

1. Introduction

Ferrocenylphosphines have emerged as a promising supporting ligand to transfer classical catalytic processes based on transition-metal complexes to aqueous media due to their capacity to incorporate several polar functional groups in the ferrocenyl backbone [1–4]. However, there are few examples in the literature of hydrophilic organometallic complexes based on ferrocenylphosphinated ligands. In this regard, we recently reported the synthesis of novel ferrocenylphosphino sulfonate ligands, their coordination, and catalytic capabilities in aqueous media [5,6] with promising results. Additionally, Štěpnička and coworkers also reported the synthesis and use of ferrocenylphosphine-amide sulfonates as ligands for hydroformylation reactions in aqueous media within good catalytic conversions [7].

Nevertheless, constant research is needed to improve known ligand structures and develop new synthetic methods. Recent works have highlighted the use of ferrocenylphosphine ligands bearing non-classical polar functional groups for catalysis in polar solvent media such as guanidinium pendants [8] and amide-sulfonate groups [9] with good catalytic activity, but also achieving good enantiomeric excess due to the incorporation of chiral fragments such as amino-oxazoline pendants [10], amine-sulfates [11,12], amino acid groups [13], amino-alcohol [14] and thio-amines [15]. The introduction of chiral polar groups to the ferrocenyl backbone represents a powerful synthetic strategy to achieve new hydrophilic ferrocenylphosphine ligands with chiral properties active in catalysis. However, the synthesis of these species has certain drawbacks, such as the use of expensive chemicals and the separation of enantiomers.

For this purpose, amino acids emerge not only as an inexpensive group suitable to provide a hydrophilic character to the ferrocenyl backbone but also as an enantiomerically pure chiral moiety, suitable to achieve chiral ferrocenyl ligands. In this regard, Štěpnička and

* Corresponding author.
E-mail address: diego.sierra@uv.cl (D. Sierra).

https://doi.org/10.1016/j.jorganchem.2025.123829
Received 13 June 2025; Received in revised form 17 August 2025; Accepted 19 August 2025
Available online 20 August 2025
0022-328X/© 2025 Elsevier B.V. All rights are reserved, including those for text and data mining, AI training, and similar technologies.

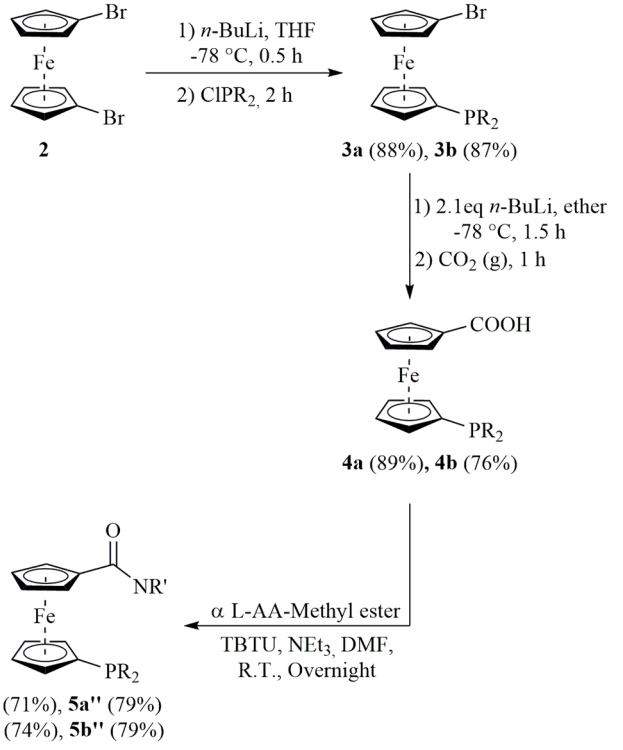
coworkers first reported the coupling of glycine pendant groups [16], as well as amino acid-protected pendant groups [17], to the preparation of a series of ferrocenylphosphine carboxamides and their catalytic activity in polar solvent media. This type of ferrocenylphosphine-amino acid ligands has also been studied for asymmetric allylic substitutions [18], oxidation of secondary alcohols [19], as well as cytotoxic agents [20, 21].

The synthetic approach for these ligands used the readily accessible 1′-diphenylphosphinoferrocenecarboxylic acid (Hdpf) [22] with standard amide coupling procedure. This method has demonstrated a versatile way to obtain enantiomerically pure ligands avoiding stereospecific synthetic processes or separations of racemic mixtures. However, the application for these ligands in organometallic chemistry is far from being completely explored and there is much research space. With these precedents in mind, herein is reported the synthesis of a group of ferrocenylphosphine-amino acid ligands (Fig. 1) by introducing two chiral amino acids methyl protected groups, proline and glutamic acid, to the corresponding 1′-diphosphinoferrocenecarboxylic acids through an alternative amide coupling procedure (Scheme 1), as well as their structural characterization. It is also reported their coordinative capabilities evaluated towards ruthenium (II) complexes and the characterization of four neutral and three cationic ruthenium (II) complexes.

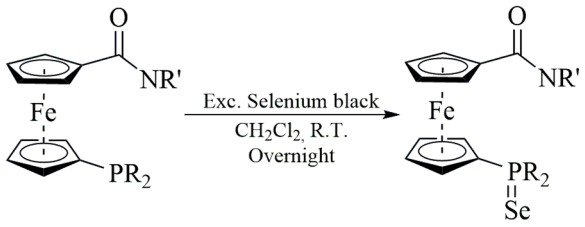
2. Experimental

2.1. General information

All reactions were performed under an argon atmosphere using standard Schlenk techniques. All chemicals were purchased from commercial sources and used as received unless otherwise indicated. 1,1′-dibromoferrocene (2) [23], 1-bromo,1′-diphenylphosphineferrocene (**3a**), 1-bromo, 1′-dicyclohexylphosphineferrocene (**3b**) [24], and dichloro(*p*-cymene)ruthenium(II) dimer (**I**) [25], were synthesized as previously reported. Anhydrous THF and ether were purified under



Scheme 1. Synthetic Pathway for the Obtention of Ferrocenylphosphine-amino acid Ligands. *R*= Ph (**a**), Cy (**b**); TBTU= *o*-Benzotriazol-1-yl-N,N,N',N'-tetramethyluronium tetrafluoroborate; AA, R'= Glu(OMe)$_2$ (’), Pro(OMe) (’’).



Scheme 2. Synthesis of Phosphine Selenides **5a’^{Se}–b’’^{Se}**. *R*= Ph (**a**), Cy (**b**); R'= Glu(OMe)$_2$ (’), Pro(OMe) (’’).

reflux with sodium metal/ benzophenone. Anhydrous dichloromethane was purified under reflux with CaH_2. Triethylamine was distilled under reduced pressure. Solvents for chromatography were ACS grade and used without additional purification.

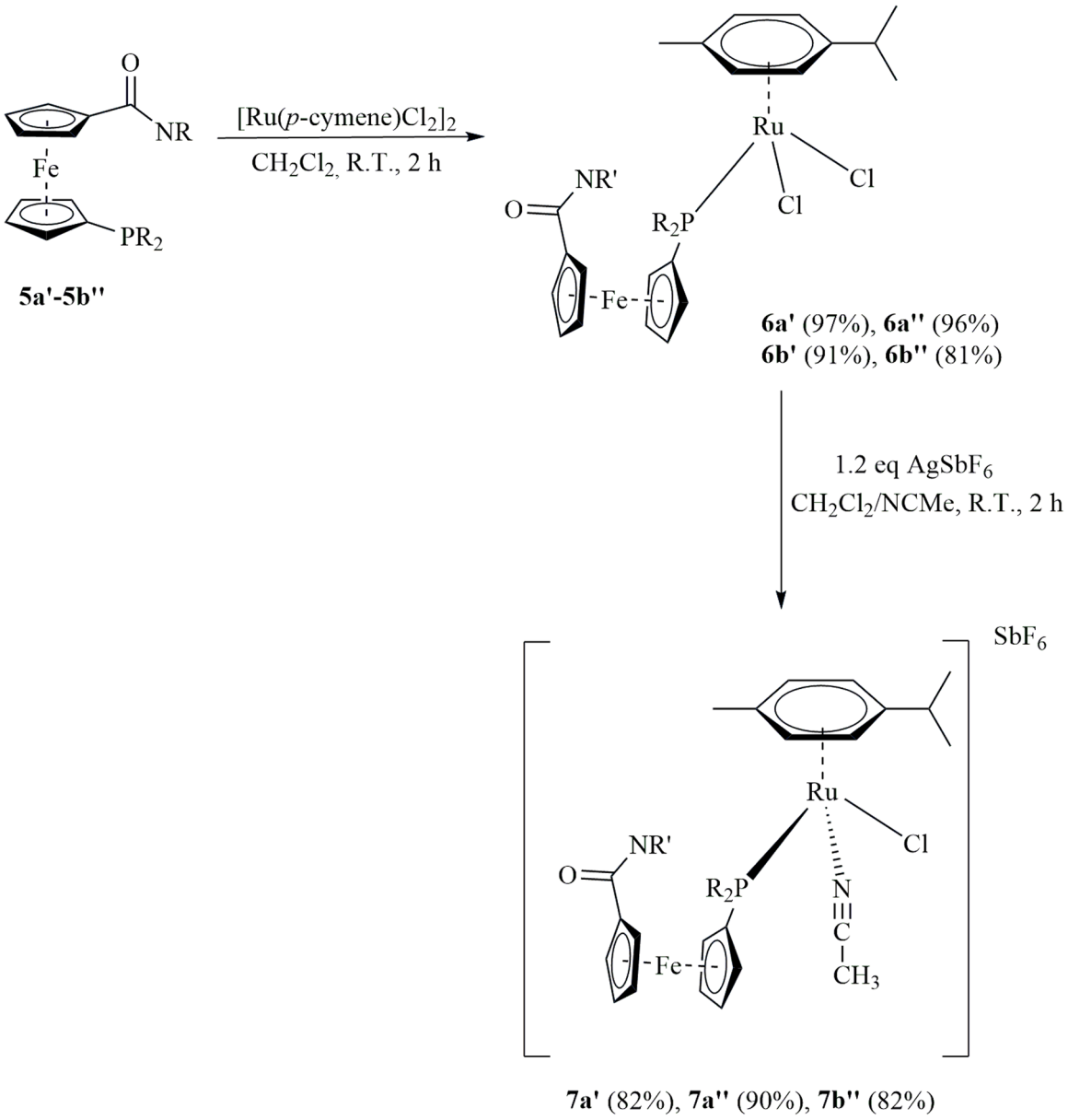
NMR spectra were recorded on Bruker NAV-300 and Bruker Avance 400 at 25 °C. Calibration of chemical shifts (δ/ppm) was made on residual signals of deuterated solvents (^{1}H: $CDCl_3$, 7.26 ppm; ^{13}C: $CDCl_3$, 77.0 ppm) or to external 85 % aqueous H_3PO_4 ($\delta_p = 0$). High-resolution mass spectra (HRMS) were carried out by ESI+ using a Bruker Impact II Micro TOF Q spectrometer.

2.2. Synthesis of 1′-diphenylphosphinoferrocenecarboxylic acid (η^5-C_5H_4-PPh_2)Fe(η^5-C_5H_4-COOH) (4a)

In a 250 mL 3-neck round bottom flask, 1.500 g of **3a** (3.34 mmol) and 120 mL of anhydrous ether were added and cooled at −78 °C. 2.81 mL of a solution of n-BuLi 2.5 M in hexanes (7.017 mmol, 2.1 eq) were added dropwise, maintaining the temperature for 30 min. The cooling was stopped for 30 min, until −50 °C, the temperature was kept for 10 min, and the solution was cooled again at −70 °C. Gaseous CO_2 was injected and bubbled into the stirring mixture for 1 h, where the cooling was suspended. The CO_2 was retired, and the solvent was removed under vacuum. The yellow solid obtained was washed with portions of hexane and dried under vacuum. The resulting solid was treated with a hot 50 % acetic acid aqueous solution. The suspension was filtered off and the orange solid was washed with water and redissolved with CH_2Cl_2. The solvent was dried over $MgSO_4$, filtered, and reduced under vacuum. An orange solid was obtained. Yield: 1.23 g, 89 %. According to NMR spectra, the compound contained some traces of the precursors (ca. 4 %). ^{1}H NMR (300 MHz, $CDCl_3$) δ 7.39 – 7.29 (m, 10H, pH), 4.76 (t, J = 2.0 Hz, 2H, cp), 4.45 (t, J = 1.8 Hz, 2H, cp), 4.34 (t, J = 2.0 Hz, 2H, cp), 4.18 (q, J = 1.8 Hz, 2H, cp). ^{31}P{^{1}H} NMR (121 MHz, $CDCl_3$) δ −18.1.

2.3. Synthesis of 1′-dicyclohexylphosphinoferrocenecarboxylic acid (η^5-C_5H_4-PCy_2)Fe(η^5-C_5H_4-COOH) (4b)

In a 250 mL 3-neck round bottom flask, 1.5 g of **3b** (3.25 mmol) and 150 mL of anhydrous ether was added and cooled at −78 °C. 2.74 mL of a solution of n-BuLi 2.5 M in hexanes (6.83 mmol, 2.1 eq) were added dropwise, maintaining the temperature for 30 min. The cooling was stopped for 30 min, until −50 °C, which was kept for 1 h, and the solution was cooled again to −70 °C. Gaseous CO_2 was injected and bubbled into the stirring mixture for 1 h, where the cooling was suspended. The CO_2 was retired, and the solvent is removed under vacuum. The pale-orange solid obtained was washed with portions of hexane and dried under vacuum. The solid was treated with a hot 75 % acetic acid aqueous solution. The resulting red solution was neutralized with a saturated $NaHCO_3$ aqueous solution until an orange suspension was obtained. The suspension was filtered off and the orange-yellow solid was washed with water and redissolved with CH_2Cl_2. The solvent was dried over $MgSO_4$, filtered, and reduced under vacuum. An orange-



Scheme 3. Synthesis of bimetallic complexes **6a'–b''** and **7a'–b''**. *R*= Ph (**a**), Cy (**b**); R'= Glu(OMe)$_2$ ('), Pro(OMe) ('').

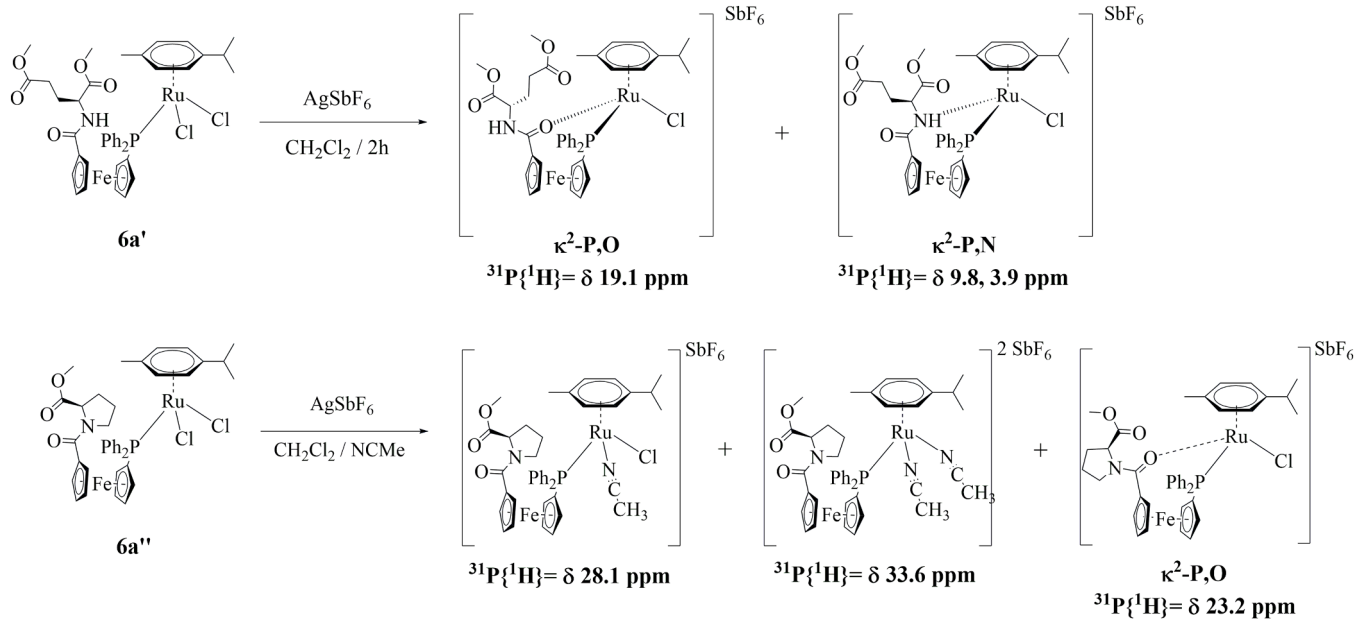
yellow solid was obtained. Yield: 1.06 g, 76 %. According to NMR spectra, the compound contained some impurities (ca. 7 %) most likely phosphine oxides [26]. ^{1}H NMR (300 MHz, $CDCl_3$) δ 4.82 (br s, 2H, cp), 4.42 (br s, 2H, cp), 4.38 (br s, 2H, cp), 4.25 (br s, 2H, cp), 1.90 (d, J = 13.0 Hz, 2H, Cy), 1.83 – 1.61 (m, 10H, Cy), 1.37 – 0.99 (m, 10H, Cy). ^{31}P{^{1}H} NMR (121 MHz, $CDCl_3$) δ −8.1.

2.4. General procedure for the synthesis of diphosphineferrocene-amino acid ligands (S)-(η^5-C_5H_4-PR_2)Fe(η^5-C_5H_4-AA) (5)

In a Schlenk tube, ferrocenylphosphinecarboxylic acid (**4a,b**), TBTU (1 eq) and AA (glutamic acid dimethyl ester, proline methyl ester) (1 eq) were added and dried under vacuum for 30 min. Excess of NEt_3 (20 eq, 4 mL) and anhydrous DMF (20 mL) were added under argon atmosphere and stirred overnight at room temperature, covered from the light. A saturated solution of $NaHCO_3$ (20 mL) was added to neutralize the reaction mixture and the product was extracted with 60 mL of ethyl acetate. The aqueous extract was washed with 2 portions of 10 mL of ethyl acetate and the organic layer was combined with the previous organic extract. The combine organic extract was washed with 200 mL of water and brine, dried over Na_2SO_4 and the solvent was reduced in vacuo. The red-orange solid obtained was purified by silica-gel column using a mixture of ethyl acetate/dichloromethane (1:2 v/v) as eluent. The first orange band was collected and reduced in vacuo. Yield: 71 – 79 %.

2.4.1. Synthesis of 1-dimethylformylglutamate, 1′-diphenylphosphineferrocene (S)-(η^5-C_5H_4-PPh_2)Fe[η^5-C_5H_4-Glu(OMe)$_2$] (5a')

Ligand (**5a'**). Starting from **4a** (575 mg, 1.39 mmol) following the general procedure. **5a'** was isolated as an orange solid. Yield: 563 mg, 71 %. ^{1}H NMR (300 MHz, $CDCl_3$) δ 7.41 – 7.29 (m, 10H, Ph), 6.61 (d, J = 7.7 Hz, 1H, NH), 4.69 (dt, J = 8.0, 4.1 Hz, 1H, CH), 4.65 (dt, J = 2.7, 1.4 Hz, 1H, cp), 4.57 (dt, J = 2.6, 1.4 Hz, 1H, cp), 4.49 (td, J = 2.4, 1.2 Hz, 1H, cp), 4.45 (td, J = 2.5, 1.2 Hz, 1H, cp), 4.26 – 4.19 (m, 3H, cp), 4.12 – 4.09 (m, 1H, cp), 3.73 (s, 3H, OMe), 3.65 (s, 3H, OMe), 2.58 – 2.37 (m, 2H, CH_2-α C = O), 2.26 (ddt, J = 14.3, 7.1, 4.8 Hz, 1H, CH_2-α CH), 2.08 (ddt, J = 14.2, 8.5, 7.1 Hz, 1H, CH_2-α CH). ^{13}C{^{1}H} NMR (75 MHz, $CDCl_3$) δ 173.6 (C = O ester), 172.3 (C = O ester), 170.0 (C = O amide),



Scheme 4. Coordination modes proposed for the bidentate coordination for ligands **5a'** (top) and **5a''** (bottom) in the formation of the ruthenium-arene cationic complexes containing the ferrocenylphosphine-amino acid ligands.

138.5 (d, $J_{P,C}$ = 9.6 Hz, Ph – P, C_{ipso}) 138.3 (d, $J_{P,C}$ = 9.3 Hz, Ph – P, C_{ipso}), 133.5 (d, $J_{P,C}$ = 5.7 Hz, Ph – P), 133.2 (d, $J_{P,C}$ = 5.7 Hz, Ph – P), 128.6 (d, $J_{P,C}$ = 3.0 Hz, Ph – P), 128.2 (d, $J_{P,C}$ = 6.8 Hz, Ph – P), 75.6 (cp, C – CONH), 74.4 (cp), 74.2 (cp), 74.0 (cp), 73.0 (d, $J_{P,C}$ = 3.6 Hz, cp), 72.9 (d, $J_{P,C}$ = 3.4 Hz, cp), 71.9 (d, $J_{P,C}$ = 4.3 Hz, cp), 69.4 (cp), 69.2 (cp), 52.4 (OMe), 51.8 (OMe), 51.7 (CH), 30.3 (CH_2-α *C* = *O*), 26.9 (CH_2-α CH); the signal due to C – P of cp was not found. $^{31}P\{^1H\}$ NMR (121 MHz, $CDCl_3$) δ −17.8. HRMS (ESI+): calculated for $C_{30}H_{31}FeNO_5P$ [*M* + *H*]$^+$ 572.1284, found 572.1296.

2.4.2. Synthesis of 1-dimethylformylglutamate, 1′-dyciclohexylphosphineferrocene (S)-(η^5-C_5H_4-PPCy$_2$)Fe[η^5-C_5H_4-Glu(OMe)$_2$] (5b')

Ligand (**5b'**). Starting from **4b** (575 mg, 1.35 mmol) following the general procedure. **5b'** was isolated as a pale orange solid. Yield: 586 mg, 74 %. ^{1}H NMR (300 MHz, $CDCl_3$) δ 6.85 (d, *J* = 7.7 Hz, 1H, NH), 4.69 – 4.59 [m, 2H: 1H, cp + 1H, CH-α N], 4.54 (br s, 1H, cp), 4.40 (br s, 1H, cp), 4.35 (br s, 2H, cp), 4.30 (br s, 2H, cp), 4.17 (br s, 1H, cp), 3.78 (s, 3H, OMe), 3.68 (s, 3H, OMe), 2.62 – 2.40 (m, 2H, CH_2-α *C* = *O*), 2.28 (ddt, *J* = 14.3, 7.3, 4.9 Hz, 1H, CH_2-α CH), 2.14 (dt, *J* = 14.5, 7.5 Hz, 1H, CH_2-α CH), 2.02 – 1.92 (m, 1H, Cy), 1.85 – 1.58 (m, 10H, Cy), 1.35 – 0.97 (m, 11H, Cy). $^{13}C\{^1H\}$ NMR (75 MHz, $CDCl_3$) δ 173.5 (*C* = *O* ester), 172.5 (*C* = *O* ester), 170.6 (*C* = *O* amide), 75.7 (cp, C – CONH), 73.4 (d, $J_{P,C}$ = 12.3 Hz, cp), 72.3 (d, $J_{P,C}$ = 7.8 Hz, cp), 72.0 (cp), 71.6 (d, $J_{P,C}$ = 3.2 Hz, cp), 71.3 (d, $J_{P,C}$ = 2.1 Hz, cp), 69.9 (cp), 69.4 (cp), 52.4 (OMe), 52.0 (CH-α N), 51.8 (OMe), 33.4 (d, $J_{P,C}$ = 11.4 Hz, CH- Cy), 33.1 (d, $J_{P,C}$ = 10.7 Hz, CH- Cy), 30.5 (CH_2- Cy), 30.4 (CH_2-α *C* = *O*), 30.2 (CH_2- Cy), 30.0 (d, $J_{P,C}$ = 4.0 Hz, CH_2- Cy), 29.8 (CH_2- Cy), 29.7 (CH_2- Cy), 27.4 (CH_2- Cy), 27.2 (d, $J_{P,C}$ = 4.3 Hz, CH_2- Cy), 27.1 (d, $J_{P,C}$ = 3.3 Hz, CH_2- Cy), 26.7 (CH_2-α CH), 26.3 (d, $J_{P,C}$ = 2.5 Hz, CH_2- Cy); the signal due to C – P of cp was not found. $^{31}P\{^1H\}$ NMR (121 MHz, $CDCl_3$) δ −8.8. HRMS (ESI+): calculated for $C_{30}H_{43}FeNO_5P$ [*M* + *H*]$^+$ 584.2223, found 584.2222.

2.4.3. Synthesis of 1-methylformylprolinate, 1′-diphenylphosphineferrocene (S)-(η^5-C_5H_4-PPh$_2$)Fe[η^5-C_5H_4-Pro(OMe)] (5a'')

Ligand (**5a''**). Starting from **4a** (550 mg, 1.33 mmol) following the general procedure. **5a''** was isolated as a red-orange solid. Yield: 553 mg, 79 %. ^{1}H NMR (300 MHz, $CDCl_3$) δ 7.38 – 7.27 (m, 10H, Ph), 4.76 (br s, 1H, cp), 4.61 – 4.54 [m, 2H: 1H, CH + 1H cp], 4.53 – 4.49 (m, 2H, cp), 4.24 (br s, 1H, cp), 4.21 (br s, 1H, cp), 4.15 – 4.08 (m, 1H, cp), 3.83 – 3.76 (m, 1H, CH_2-α N), 3.74 (s, 3H, OMe), 3.70 – 3.63 (m, 1H, CH_2-α N), 2.26 – 2.04 (m, 2H, CH_2-β *C* = *O*, partly overlapping with residual ethyl acetate), 2.00 – 1.91 (m, 2H, CH_2-γ *C* = *O*). $^{13}C\{^1H\}$ NMR (75 MHz, $CDCl_3$) δ 172.8 (*C* = *O* ester), 168.9 (*C* = *O* amide), 138.7 (d, $J_{P,C}$ = 10.5 Hz, Ph – P, C_{ipso}), 133.5 (Ph – P), 133.2 (Ph – P), 128.5 (d, $J_{P,C}$ = 3.0 Hz, Ph – P), 128.1 (d, $J_{P,C}$ = 6.9 Hz, Ph – P), 76.3 (cp, C – CONH), 74.1 (cp,), 73.9 (cp), 73.4 (d, $J_{P,C}$ = 3.9 Hz, cp), 73.3 (d, $J_{P,C}$ = 3.4 Hz, cp), 72.1 (cp), 71.8 (cp), 70.7 (cp), 60.1 (CH), 52.1 (OMe), 48.1 (CH_2-α N), 28.5 (CH_2-β *C* = *O*), 25.4 (CH_2-γ *C* = *O*); the signal due to C – P of cp was not found. $^{31}P\{^1H\}$ NMR (121 MHz, $CDCl_3$) δ −17.6. HRMS (ESI+): calculated for $C_{29}H_{29}FeNO_3P$ [*M* + *H*]$^+$ 526.1229, found 526.1240.

2.4.4. Synthesis of 1-methylformylprolinate, 1′-dicyclohexylphosphineferrocene (S)-(η^5-C_5H_4-PCy$_2$)Fe[η^5-C_5H_4-Pro(OMe)] (5b'')

Ligand (**5b''**). Starting from **4b** (576 mg, 1.35 mmol) following the general procedure. **5b''** was isolated as a pale orange solid. Yield: 575 mg, 79 %. ^{1}H NMR (300 MHz, $CDCl_3$) δ 4.81 (br s, 1H, cp), 4.69 (br s, 1H, cp), 4.59 (dd, *J* = 8.0, 4.5 Hz, 1H, CH-α N), 4.42 (br s, 2H, cp), 4.29 (br s, 2H, cp), 4.24 (br s, 1H, cp), 4.19 (br s, 1H, cp), 3.95 (q, *J* = 6.0, 4.8 Hz, 1H, CH_2-α N), 3.83 – 3.68 [m, 4H: 1H, CH_2-α *N* + 3H, OMe], 2.28 – 2.06 (m, 2H, CH_2-β *C* = *O*), 2.05 – 1.90 (m, 2H, CH_2-γ *C* = *O*), 1.89 – 1.57 (m, 10H, Cy), 1.37 – 0.91 (m, 12H, Cy). $^{13}C\{^1H\}$ NMR (75 MHz, $CDCl_3$) δ 172.8 (*C* = *O* ester), 169.3 (*C* = *O* amide), 76.0 (cp, C – CONH), 72.7 (cp), 72.5 (d, $J_{P,C}$ = 7.1 Hz, cp) 72.3 (d, $J_{P,C}$ = 6.1 Hz, cp), 71.7 (d, $J_{P,C}$ = 2.6 Hz, cp), 70.5 (cp), 60.1 (CH-α N), 52.0 (OMe), 48.2 (CH_2-α N), 33.2 (d, $J_{P,C}$ = 11.8 Hz, CH- Cy), 33.0 (d, $J_{P,C}$ = 11.1 Hz, CH- Cy), 30.2 (d, $J_{P,C}$ = 2.7 Hz, CH_2- Cy), 30.0 (d, $J_{P,C}$ = 5.9 Hz, CH_2- Cy), 29.8 (d, $J_{P,C}$ = 2.9 Hz, CH_2- Cy), 29.7 (CH_2- Cy), 28.6 (CH_2-β *C* = *O*), 27.3 (d, $J_{P,C}$ = 4.2 Hz, CH_2- Cy), 27.2 (d, $J_{P,C}$ = 3.4 Hz, CH_2- Cy), 27.1 (d, $J_{P,C}$ = 2.1 Hz, CH_2- Cy), 26.3 (CH_2- Cy), 25.5 (CH_2-γ *C* = *O*); the signal due to C – P of cp was not found. $^{31}P\{^1H\}$ NMR (121 MHz, $CDCl_3$) δ −8.2. HRMS (ESI+): calculated for $C_{29}H_{41}FeNO_3P$ [*M* + *H*]$^+$ 538.2168, found 538.2164.

2.5. General procedure for the synthesis of selenium oxides from ligands (S)-(η^5-C_5H_4-PSeR$_2$)Fe(η^5-C_5H_4-AA) (5^{Se})

In a Schlenk tube, ligands **5a'**–**b''** and excess of selenium black were added and dissolved in 10 mL of anhydrous dichloromethane. The

suspension was stirred at room temperature overnight. Then, the stirring was stopped, and the suspension was filtered off through celite and the solvent was reduced under vacuum. The orange oily solid was redissolved in ether and dried under vacuum to obtain the selenides in quantitative yields.

2.5.1. Synthesis of selenium oxide (S)-(η^5-C_5H_4-PSePPh$_2$)Fe[η^5-C_5H_4-Glu(OMe)$_2$] (5a'^{Se})

Complex (**5a'^{Se}**). Starting from **5a'** (46.8 mg, 0.082 mmol) and excess of selenium black (127 mg, 1.61 mmol) following the general procedure. An orange solid was obtained. $^{31}P\{^1H\}$ NMR (162 MHz, $CDCl_3$) δ 31.8 (with satellite signals of ^{77}Se, $^1J_{PSe}$= 721.9 Hz).

2.5.2. Synthesis of selenium oxide (S)-(η^5-C_5H_4-PSePCy$_2$)Fe[η^5-C_5H_4-Glu(OMe)$_2$] (5b'^{Se})

Complex (**5b'^{Se}**). Starting from **5b'** (50 mg, 0.086 mmol) and excess of selenium black (104 mg, 1.32 mmol) following the general procedure. An orange solid was obtained. $^{31}P\{^1H\}$ NMR (162 MHz, $CDCl_3$) δ 50.0 (with satellite signals of ^{77}Se, $^1J_{PSe}$= 687.4 Hz).

2.5.3. Synthesis of selenium oxide (S)-(η^5-C_5H_4-PSePPh$_2$)Fe[η^5-C_5H_4-Pro(OMe)] (5a''^{Se})

Complex (**5a''^{Se}**). Starting from **5a''** (49.6 mg, 0.094 mmol) and excess of selenium black (107 mg, 1.36 mmol) following the general procedure. An orange solid was obtained. $^{31}P\{^1H\}$ NMR (162 MHz, $CDCl_3$) δ 31.3 (with satellite signals of ^{77}Se, $^1J_{PSe}$= 735.0 Hz).

2.5.4. Synthesis of selenium oxide (S)-(η^5-C_5H_4-PSePCy$_2$)Fe[η^5-C_5H_4-Pro(OMe)] (5b''^{Se})

Complex (**5b''^{Se}**). Starting from **5b''** (50 mg, 0.093 mmol) and excess of selenium black (105 mg, 1.33 mmol) following the general procedure. An orange solid was obtained. $^{31}P\{^1H\}$ NMR (162 MHz, $CDCl_3$) δ 49.5 (with satellite signals of ^{77}Se, $^1J_{PSe}$= 700.6 Hz).

2.6. General procedure for the synthesis of neutral dichloro(p-cymene)(diphosphineferrocene-amino acid)ruthenium (II) complexes RuCl$_2$(η^6-$C_{10}H_{14}$) {PR$_2$-[(η^5-C_5H_4)Fe(η^5-C_5H_4-AA)]} (6)

In a Schlenk tube, dichloro(*p*-cymene)ruthenium(II) dimer (**I**) and 2 eq of the corresponding diphosphineferrocene-amino acid ligand (**5a'**–b'') were added and dried under vacuum for 30 min. 10 mL of anhydrous CH_2Cl_2 were added and the mixture was stirred for 2 h under argon atmosphere. The solvent was reduced to a 2 mL volume and hexane was added until a red-orange suspension was formed. The solid was decanted, washed with three portions of hexane, and dried under vacuum. A red-orange powder solid was obtained. Yield: 81 – 97 %.

2.6.1. Synthesis of complex dichloro(p-cymene)(1-dimethylformylglutamate,1′-diphenylphosphineferrocene)ruthenium (II) RuCl$_2$(η^6-$C_{10}H_{14}$){PPh$_2$-[(η^5-C_5H_4)Fe(η^5-C_5H_4-Glu(OMe)$_2$]} (6a')

Complex (**6a'**). Starting from **I** (100.0 mg, 0.163 mmol) and **5a'** (191.2 mg, 0.33 mmol) following the general procedure. **6a'** was isolated as a red-orange powder solid. Yield: 284 mg, 97 %. ^1H NMR (300 MHz, $CDCl_3$) δ 7.87 (td, J = 8.1, 3.8 Hz, 2H, Ph – P), 7.70 (td, J = 7.9, 3.8 Hz, 2H, Ph – P), 7.50 (d, J = 8.2 Hz, 1H, NH), 7.44 – 7.35 (m, 6H, Ph – P), 5.29 (br s, 1H, Ph, *p*-cym), 5.23 (d, J = 6.0 Hz, 1H, Ph, *p*-cym), 5.15 (d, J = 6.1 Hz, 1H, Ph, *p*-cym), 4.88 (br s, 1H, cp), 4.80 (d, J = 6.2 Hz, 1H, Ph, *p*-cym), 4.61 – 4.43 [m, 5H: 1H, CH-α *N* + 4H cp], 4.36 (br s, 1H, cp), 3.78 (s, 3H, OMe), 3.71 – 3.64 [m, 4H: 1H cp + 3H OMe], 2.90 (s, 1H, cp), 2.67 – 2.42 (m, 3H: 1H, CH – *i*-pr, *p*-cym + 2H, CH_2-α *C* = *O*), 2.39 – 2.23 (m, 2H, CH_2-α CH), 1.69 (s, 3H, CH_3, *p*-cym), 1.04 (d, J = 6.9 Hz, 6H, CH_3 – *i*-pr, *p*-cym). $^{13}C\{^1H\}$ NMR (75 MHz, $CDCl_3$) δ 173.3 (*C* = *O* ester), 172.8 (*C* = *O* ester), 170.4 (*C* = *O* amide), 138.2 (d, $J_{P,C}$ = 47.4 Hz, Ph – P, C_{ipso}), 135,6 (d, $J_{P,C}$ = 49.6 Hz, Ph – P, C_{ipso}), 134.5 (d, $J_{P,C}$ = 9.4 Hz, Ph – P) 133.0 (d, $J_{P,C}$ = 9.2 Hz, Ph – P), 130.0 (d, $J_{P,C}$ = 11.5 Hz, Ph – P), 127.7 (d, $J_{P,C}$ = 9.9 Hz, Ph – P), 127.4 (d, $J_{P,C}$ = 9.7 Hz, Ph – P), 111.2 (Ph, C_{ipso}, *p*-cym), 97.2 (Ph, C_{ipso}, *p*-cym), 88.5 (Ph, *p*-cym), 87.4 (d, $J_{P,C}$ = 8.5 Hz, Ph, *p*-cym), 86.7 (d, $J_{P,C}$ = 5.0 Hz, Ph, *p*-cym), 79.3 (d, $J_{P,C}$ = 15.3 Hz, cp), 77.8 (C – CONH, cp, partly overlapping with the solvent signal), 74.4 (d, $J_{P,C}$ = 5.9 Hz, cp), 72.8 (cp), 72.7 (d, $J_{P,C}$ = 6.6 Hz, cp), 72.6 (cp), 72.1 (cp), 71.9 (d, $J_{P,C}$ = 8.9 Hz, cp), 69.5 (cp), 52.2 (OMe), 52.1 (CH-α N), 51.7 (OMe), 30.6 (CH_2-α *C* = *O*), 29.8 (CH – *i*-pr, *p*-cym), 26.2 (CH_2-α CH), 22.1 (CH_3 – *i*-pr, p-cym), 21.3 (CH_3 – *i*-pr, p-cym), 17.1 (CH_3, *p*-cym); the signal due to C – P of cp was not found. $^{31}P\{^1H\}$ NMR (121 MHz, $CDCl_3$) δ 17.5; a signal was observed at δ 30.4 ppm (ca. 3 %) attributed to the corresponding phosphine oxide of the free ligand. MS (ESI+): *m/z* 842 ($[M - Cl]^+$).

2.6.2. Synthesis of complex dichloro(p-cymene)(1-dimethylformylglutamate,1′-dicyclohexylphosphineferrocene)ruthenium (II) RuCl$_2$(η^6-$C_{10}H_{14}$){PCy$_2$-[(η^5-C_5H_4)Fe(η^5-C_5H_4-Glu(OMe)$_2$]} (6b')

Complex (**6b'**). Starting from **I** (52.5 mg, 0.086 mmol) and **5b'** (100 mg, 0.172 mmol) following the general procedure. **6b'** was isolated as a red-orange powder solid. Yield: 138 mg, 91 %. ^1H NMR (300 MHz, $CDCl_3$) δ 7.05 (d, J = 7.0 Hz, 1H, NH), 5.01 (t, J = 6.6 Hz, 2H, Ph, *p*-cym), 4.92 (d, J = 5.4 Hz, 1H, Ph, *p*-cym), 4.87 (br s, 2H: 1H Ph, p-cym + 1H cp), 4.76 (s, 1H, cp), 4.70 – 4.61 [m, 4H: 1H CH-α *N* + 3H cp], 4.59 (br s, 1H, cp), 4.44 (br s, 2H, cp), 3.81 (s, 3H, OMe), 3.72 (s, 3H, OMe), 2.73 – 2.60 (m, 1H, CH – *i*-pr, *p*-cym), 2.58 – 2.44 [m, 3H: 1H Cy + 2H CH_2-α *C* = *O*], 2.42 – 2.07 [m, 6H: 4H, Cy + 2H, CH_2-α CH], 2.01 – 1.79 [m, 8H: 3H, CH_3, *p*-cym + 5H, Cy), 1.78 – 1.62 (m, 4H, Cy), 1.41 – 1.18 (m, 8H, Cy), 1.14 (d, J = 6.8 Hz, 6H, CH_3 – *i*-pr, p-cym). $^{13}C\{^1H\}$ NMR (75 MHz, CDCl3) δ 174.2 (*C* = *O* ester), 172.3 (*C* = *O* ester), 169.4 (*C* = *O* amide), 107.2 (Ph, C_{ipso}, *p*-cym), 93.9 (Ph, C_{ipso}, *p*-cym), 89.6 (Ph, *p*-cym), 89.4 (d, $J_{P,C}$ = 3.8 Hz, Ph, *p*-cym), 85.1 (d, $J_{P,C}$ = 4.4 Hz, Ph, *p*-cym), 82.2 (d, $J_{P,C}$ = 28.2 Hz, C – P, cp), 75.9 (C – CONH, cp), 73.8 (d, $J_{P,C}$ = 8.7 Hz, cp), 73.3 (d, $J_{P,C}$ = 7.6 Hz, cp), 73.2 (d, $J_{P,C}$ = 5.9 Hz, cp), 72.2 (unresolved dd, cp), 70.1 (cp), 69.1 (cp), 52.5 (OMe), 52.1 (CH-α N), 52.0 (OMe), 39.7 (d, $J_{P,C}$ = 10.3 Hz, CH- Cy) 39.4 (d, $J_{P,C}$ = 9.9 Hz, CH- Cy), 30.4 (CH_2-α *C* = *O*), 30.3 (CH – *i*-pr, *p*-cym), 29.7 (Cy), 29.1 (Cy), 27.8 (d, $J_{P,C}$ = 6.3 Hz, Cy), 27.7 (d, $J_{P,C}$ = 6.7 Hz, Cy), 26.1 (CH_2-α CH), 26.0 (Cy), 22.3 (CH_3 – *i*-pr, *p*-cym), 22.2 (CH_3 – *i*-pr, *p*-cym), 17.6 (CH_3, *p*-cym). $^{31}P\{1H\}$ NMR (121 MHz, $CDCl_3$) δ 17.4; a signal was observed at δ 47.4 ppm (< 1 %) attributed to the corresponding phosphine oxide of the free ligand. MS (ESI+): *m/z* 854 ($[M - Cl]^+$).

2.6.3. Synthesis of complex dichloro(p-cymene)(1-methylformylprolinate,1′-diphenylphosphineferrocene)rutenio (II) RuCl$_2$(η^6-$C_{10}H_{14}$){PPh$_2$-[(η^5-C_5H_4)Fe(η^5-C_5H_4-Pro(OMe)]} (6a'')

Complex (**6a''**). Starting from **I** (100.0 mg, 0.163 mmol) and **5a''** (171.6 mg, 0.33 mmol) following the general procedure. 6a'' was isolated as a red-orange powder solid. Yield: 260 mg, 96 %. ^1H NMR (300 MHz, $CDCl_3$) δ 7.88 – 7.79 (m, 4H, Ph – P), 7.45 – 7.37 (m, 6H, Ph – P), 5.15 (q, J = 6.3, 5.7 Hz, 3H, Ph, *p*-cym), 5.08 (d, J = 6.1 Hz, 1H, Ph, *p*-cym), 4.64 (br s, 1H, cp), 4.57 (br s, 1H, cp), 4.54 – 4.49 [m, 2H: 1H, CH-α *N* + 1H cp], 4.46 (br s, 2H, cp), 4.33 (br s, 1H, cp), 3.79 (q, J = 2.2 Hz, 1H, cp), 3.73 (s, 3H, OMe), 3.69 – 3.65 (m, 1H, cp), 3.64 – 3.55 (m, 1H, CH_2-α N), 2.51 (sept, J = 6.5 Hz, 1H, CH – *i*-pr, *p*-cym), 2.24 – 2.13 (m, 1H, CH_2-β *C* = *O*), 2.11 – 1.98 (m, 1H, CH_2-γ *C* = *O*), 1.97 – 1.87 (m, 2H: 1H, CH_2-β *C* = *O* + 1H, CH_2-γ *C* = *O*), 1.78 (s, 3H, CH_3, *p*-cym), 0.95 (d, J = 6.9 Hz, 3H, CH_3 – *i*-pr, p-cym), 0.91 (d, J = 6.9 Hz, 3H, CH_3 – *i*-pr, p-cym); the signal due to 1H of CH_2-α N was not found. However, the 2D-HSQC experiment showed that the signal is overlapped with the singlet signal of the OMe group at δ 3.72 ppm (See Figure S39).$^{13}C\{^1H\}$ NMR (75 MHz, $CDCl_3$) δ 172.8 (*C* = *O* ester), 168.9 (*C* = *O* amide), 136.6 (d, $J_{P,C}$ = 44.7 Hz, Ph – P, C_{ipso}), 133.8 (d, $J_{P,C}$ = 9.3 Hz, Ph – P), 130.1 (Ph – P), 127.5 (d, $J_{P,C}$ = 9.8 Hz, Ph – P), 109.5 (Ph, C_{ipso}, *p*-cym), 95.1 (Ph, C_{ipso}, *p*-cym), 90.3 (d, $J_{P,C}$ = 4.4 Hz, Ph, *p*-cym), 90.0 (d, $J_{P,C}$ = 3.9 Hz, Ph, *p*-cym), 86.0 (d, $J_{P,C}$ = 5.8 Hz, Ph, *p*-cym), 85.6 (d, $J_{P,C}$ = 5.8 Hz, Ph, *p*-cym), 77.6 (C – CONH, cp, partly overlapping with the solvent signal), 76.2 (d, $J_{P,C}$ = 5.3 Hz, cp), 76.1 (d, $J_{P,C}$ = 5.3 Hz, cp), 74.6 (cp), 73.3 (cp), 73.1 (d, $J_{P,C}$ = 7.8 Hz, cp), 72.9 (d, $J_{P,C}$ = 8.0 Hz, cp), 72.2 (cp),

71.0 (cp), 60.0 (CH-α N), 52.0 (OMe), 48.2 (CH_2-α N), 29.9 (CH – *i*-pr, p-cym), 28.6 (CH_2-β *C* = *O*), 25.4 (CH_2-γ *C* = *O*), 21.7 (CH_3 – *i*-pr, p-cym), 21.5 (CH_3 – *i*-pr, p-cym), 16.9 (CH_3, *p*-cym); the signal due to C – P of cp was not found. $^{31}P\{^1H\}$ NMR (121 MHz, $CDCl_3$) δ 18.6. MS (ESI+): *m/z* 796 ($[M - Cl]^+$).

2.6.4. Synthesis of complex dichloro(p-cymene)(1-methylformylprolinate,1′-dicyclohexylphosphineferrocene)ruthenium (II) $RuCl_2(\eta^6\text{-}C_{10}H_{14})\{PCy_2\text{-}[(\eta^5\text{-}C_5H_4)Fe(\eta^5\text{-}C_5H_4\text{-}Pro(OMe)]\}$ (6b'')

Complex (**6b''**). Starting from **I** (57 mg, 0.093 mmol) and **5b''** (100 mg, 0.186 mmol) following the general procedure. 6b'' was isolated as a red-orange powder solid. Yield: 127 mg, 81 %. ^1H NMR (300 MHz, $CDCl_3$) δ 5.01 – 4.88 (m, 4H: 3H, Ph, *p*-cym + 1H, cp), 4.81 – 4.73 (m, 2H: 1H, Ph, *p*-cym + 1H, cp), 4.70 (br s, 2H, cp), 4.64 – 4.55 [m, 3H: 1H, CH-α *N* + 2H, cp], 4.44 (br s, 2H, cp), 3.93 – 3.84 (m, 1H, CH_2-α N), 3.79 (s, 3H, OMe), 3.74 – 3.67 (m, 1H, CH_2-α N), 2.71 – 2.47 (m, 2H: 1H, CH – *i*-pr, *p*-cym + 1H, Cy), 2.46 – 2.30 (m, 4H, Cy), 2.29 – 2.08 (m, 3H: 2H, CH_2-β *C* = *O* + 1H, CH_2-γ *C* = *O*), 2.06 – 1.94 (m, 2H: 1H, CH_2-γ *C* = *O* + 1H, Cy), 1.87 (br s, 6H: 3H, CH_3, *p*-cym + 3H, Cy), 1.78 – 1.65 (m, 3H, Cy), 1.41 – 1.17 (m, 10H, Cy), 1.12 (br d, *J* = 7.0, 6H, CH_3 – *i*-pr, p-cym). $^{13}C\{^1H\}$ NMR (75 MHz, $CDCl_3$) δ 172.7 (*C* = *O* ester), 168.5 (*C* = *O* amide), 107.0 (Ph, C_{ipso}, *p*-cym), 93.9 (Ph, C_{ipso}, *p*-cym), 89.8 (d, $J_{P,C}$ = 3.2 Hz, Ph, *p*-cym), 89.2 (Ph, *p*-cym), 85.2 (d, $J_{P,C}$ = 4.4 Hz, Ph, *p*-cym), 85.0 (d, $J_{P,C}$ = 5.2 Hz, Ph, *p*-cym), 82.4 (d, $J_{P,C}$ = 28.5 Hz, C – P, cp), 73.4 (d, $J_{P,C}$ = 8.8 Hz, cp), 73.2 (d, $J_{P,C}$ = 7.2 Hz, cp), 73.0 (cp), 72.8 (cp), 72.5 (d, $J_{P,C}$ = 6.5 Hz, cp), 70.6 (cp), 59.9 (CH-α N), 52.2 (OMe), 48.4 (CH_2-α N), 39.4 (d, $J_{P,C}$ = 12.7 Hz, CH- Cy), 39.2 (d, $J_{P,C}$ = 12.3 Hz, CH-Cy), 30.3 (CH – *i*-pr, p-cym), 29.8 (Cy), 29.2 (d, $J_{P,C}$ = 5.6 Hz, Cy), 28.6 (CH_2-β *C* = *O*), 27.9 (d, $J_{P,C}$ = 3.8 Hz, Cy), 27.8 (Cy), 27.7 (d, *J* = 5.7 Hz, Cy), 26.0 (Cy), 25.4 (CH_2-γ *C* = *O*), 22.3 (CH_3 – *i*-pr, p-cym), 22.1 (CH_3 – *i*-pr, p-cym), 17.5 (CH_3, *p*-cym); the signal due to C – CON of the cp was not found probably due to overlaps. $^{31}P\{^1H\}$ NMR (121 MHz, $CDCl_3$) δ 17.2. MS (ESI+): *m/z* 808 ($[M - Cl]^+$).

2.7. General procedure for the synthesis of cationic hexafluoroantimonate of dichloroacetonitril(p-cymene)(diphosphineferrocene-amino acid) ruthenium (II) complexes $\langle RuCl(NCMe)(\eta^6\text{-}C_{10}H_{14})\{PR_2\text{-}[(\eta^5\text{-}C_5H_4)Fe(\eta^5\text{-}C_5H_4\text{-}AA)]\}\rangle SbF_6$ (7)

In a Schlenk tube, 50.0 mg of dichloro(*p*-cymene)(diphosphineferrocene-amino acid)ruthenium (II) complex (**6a'–b''**) were added and dried under vacuum for 30 min. 5 mL of anhydrous CH_2Cl_2, 1 mL of degassed NCMe and 1.2 eq of $AgSbF_6$ were added under argon atmosphere, and the mixture was stirred for 1 h covered from the light and 1 h in presence of light. The mixture was filtered off through celite and the filtrate was evaporated under vacuum. The resulting orange oil was washed with portions of ether, obtaining a solid, which was dried under vacuum. An orange crystalline solid was obtained. Yields: 82 – 90 %.

2.7.1. Synthesis of complex hexafluoroantimonate of [chloroacetonitril(p-cymene)(1-dimethylformylglutamate,1′-diphenylphosphineferrocene) ruthenium (II)] $\langle RuCl(NCMe)(\eta^6\text{-}C_{10}H_{14})\{PPh_2\text{-}[(\eta^5\text{-}C_5H_4)Fe(\eta^5\text{-}C_5H_4\text{-}Glu(OMe)_2)]\}\rangle SbF_6$ (7a')

Complex (**7a'**). Starting from **6a'** (50 mg, 0.057 mmol) and $AgSbF_6$ (23.5 mg, 0.068 mmol) following the general procedure. **7a'** was isolated as an orange crystalline solid. Yield: 52 mg, 82 %. ^1H NMR (300 MHz, $CDCl_3$) δ 7.86 – 7.75 (m, 7H, Ph – P), 7.66 – 7.46 (m, 13zH, Ph – P), 7.31 (d, *J* = 8.0 Hz, 1H, NH, partly overlapping with the solvent signal), 7.00 (d, *J* = 7.8 Hz, 1H, NH), 5.77 (dd, *J* = 6.2, 1.4 Hz, 1H, Ph, *p*-cym), 5.67 (td, *J* = 6.4, 1.4 Hz, 2H, Ph, *p*-cym), 5.43 (d, *J* = 6.2 Hz, 1H, Ph, *p*-cym), 5.35 (dt, *J* = 6.2, 1.9 Hz, 2H, Ph, *p*-cym), 5.04 (t, *J* = 1.6 Hz, 1H, Ph, *p*-cym), 5.03 – 5.00 (m, 1H, cp), 4.98 – 4.96 (m, 1H, cp), 4.76 – 4.71 [m, 4H: 1 H, Ph, *p*-cym + 3H, cp], 4.71 – 4.68 (m, 2H, cp), 4.67 – 4.65 (m, 2H, cp), 4.64 – 4.57 (m, 2H, CH-α N), 4.52 – 4.48 (m, 2H, cp), 3.97 (td, *J* = 2.7, 1.3 Hz, 2H, cp), 3.93 (td, *J* = 2.5, 1.1 Hz, 1H, cp), 3.81 (unresolved dd, *J* = 2.7, 1.5 Hz, 1H, cp, partly overlapping with the OMe signal), 3.79 (s, 3H, OMe), 3.78 (s, 3H, OMe), 3.71 (s, 3H, OMe), 3.70 (s, 3H, OMe), 3.36 (q, *J* = 2.2 Hz, 1H, cp), 2.79 (quint, *J* = 6.9 Hz, 1H, CH – *i*-pr, *p*-cym), 2.67 (quint, *J* = 7.0 Hz, 1H, CH – *i*-pr, *p*-cym), 2.60 – 2.47 (m, 4H:CH_2-α *C* = *O*), 2.39 – 2.18 (m, 4H, CH_2-α CH, partly overlapping with the NCMe signal), 2.18 (d, *J* = 1.5 Hz, 3H, NCMe), 2.16 (d, *J* = 1.4 Hz, 3H, NCMe), 1.89 (s, 3H, CH_3, *p*-cym), 1.73 (s, 3H, CH_3, *p*-cym), 1.28 – 1.15 (m, 12H, CH_3 – *i*-pr, p-cym, overlapped with residual ethyl acetate). $^{13}C\{^1H\}$ NMR (75 MHz, $CDCl_3$) δ 173.8 (*C* = *O* ester), 173.6 (*C* = *O* ester), 172.9 (*C* = *O* ester), 172.3 (*C* = *O* ester), 169.5 (*C* = *O* amide), 169.3 (*C* = *O* amide), 134.7 (d, $J_{P,C}$ = 9.8 Hz, Ph – P), 134.4 (d, $J_{P,C}$ = 9.7 Hz, Ph – P), 133.5 (d, $J_{P,C}$ = 9.4 Hz, Ph – P), 133.0 (d, $J_{P,C}$ = 9.7 Hz, Ph – P), 131.9 (Ph – P), 131.5 (Ph – P), 131.3 (Ph – P), 131.0 (Ph – P), 128.7 (Ph – P), 128.5 (d, $J_{P,C}$ = 1.9 Hz, Ph – P), 128.3 (d, $J_{P,C}$ = 2.8 Hz, Ph – P), 128.2 (d, $J_{P,C}$ = 2.5 Hz, Ph – P), 128.1 (Ph – P), 116.1 (Ph, C_{ipso}, *p*-cym), 114.3 (Ph, C_{ipso}, *p*-cym), 103.0 (Ph, C_{ipso}, *p*-cym), 101.2 (Ph, C_{ipso}, *p*-cym), 91.8 (d, $J_{P,C}$ = 4.5 Hz, Ph, *p*-cym), 90.7 (d, $J_{P,C}$ = 3.0 Hz, Ph, *p*-cym), 90.1 (d, $J_{P,C}$ = 6.1 Hz, Ph, *p*-cym), 89.5 (Ph, *p*-cym), 89.2 (Ph, *p*-cym), 88.4 (Ph, *p*-cym), 88.2 (d, $J_{P,C}$ = 2.2 Hz, Ph, *p*-cym), 88.0 (Ph, *p*-cym), 77.7 (C – CONH, cp), 75.7 (cp), 75.6 (d, $J_{P,C}$ = 3.7 Hz, cp), 75.2 (d, $J_{P,C}$ = 5.5 Hz, cp), 75.0 (cp), 74.6 (d, $J_{P,C}$ = 7.3 Hz, cp), 73.9 (cp), 73.7 (d, $J_{P,C}$ = 7.3 Hz, cp), 73.1 (cp), 73.0 (d, $J_{P,C}$ = 6.3 Hz, cp), 72.6 (d, $J_{P,C}$ = 9.4 Hz, cp), 72.2 (d, $J_{P,C}$ = 8.7 Hz, cp), 72.0 (cp), 70.6 (cp), 69.7 (cp), 52.4 (OMe), 52.1 (CH-α N), 52.0 (CH-α N), 52.0 (OMe), 51.9 (OMe), 31.0 (CH – *i*-pr, *p*-cym), 31.0 (CH – *i*-pr, *p*-cym), 30.5 (CH_2-α *C* = *O*), 30.5 (CH_2-α *C* = *O*), 26.3 (CH_2-α CH), 26.2 (CH_2-α CH), 22.7 (CH_3 – *i*-pr, p-cym), 22.6 (CH_3 – *i*-pr, p-cym), 21.3 (CH_3 – *i*-pr, p-cym), 21.2 (CH_3 – *i*-pr, p-cym), 18.1 (CH_3, *p*-cym), 17.8 (CH_3, *p*-cym), 3.9 (CH_3, NCMe), 3.8 (CH_3, NCMe); the signals due to C_{ipso} of Ph – P, quaternary C of NCMe and C – P of cp were not found. $^{31}P\{^1H\}$ NMR (121 MHz, $CDCl_3$) δ 28.1, 25.9. MS (ESI+): *m/z* 842 ($[M - NCMe - SbF_6]^+$).

2.7.2. Synthesis of cationic complex hexafluoroantimonate of [chloroacetonitril(p-cymene)(1-dimethylformylglutamate,1′-dicyclohexylphosphineferrocene)ruthenium (II)] $\langle RuCl(NCMe)(\eta^6\text{-}C_{10}H_{14})\{PCy_2\text{-}[(\eta^5\text{-}C_5H_4)Fe(\eta^5\text{-}C_5H_4\text{-}Glu(OMe)_2)]\}\rangle SbF_6$ (7b')

Complex (**7b'**). Starting from **6b'** (50 mg, 0.057 mmol) and $AgSbF_6$ (23.2 mg, 0.068 mmol) following the general procedure. An orange crystalline solid was obtained. **7b'** could not be isolated in pure form and NMR analysis were not conclusive.

2.7.3. Synthesis of cationic complex hexafluoroantimonate of [chloroacetonitril(p-cymene)(1-methylformylprolinate,1′-diphenylphosphineferrocene)ruthenium (II)] $\langle RuCl(NCMe)(\eta^6\text{-}C_{10}H_{14})\{PPh_2\text{-}[(\eta^5\text{-}C_5H_4)Fe(\eta^5\text{-}C_5H_4\text{-}Pro(OMe))]\}\rangle SbF_6$ (7a'')

Complex (**7a''**). Starting from **6a''** (50 mg, 0.057 mmol) and $AgSbF_6$ (24.8 mg, 0.068 mmol) following the general procedure. **7a''** was isolated as an orange crystalline solid. Yield: 58 mg, 90 %. ^1H NMR (300 MHz, $CDCl_3$) δ 7.90 – 7.73 (m, 8H, Ph – P), 7.58 – 7.47 (m, 12H, Ph – P), 5.62 (dd, *J* = 6.2, 1.4 Hz, 1H, Ph, *p*-cym), 5.59 (dd, *J* = 6.3, 1.3 Hz, 1H, Ph, *p*-cym) 5.37 (dd, *J* = 6.4, 4.9, 1.4 Hz, 2H, Ph, *p*-cym), 5.32 – 5.25 (m, 2H, Ph, *p*-cym), 5.18 (dt, *J* = 6.2, 1.5 Hz, 1H, Ph, *p*-cym), 5.11 (dt, *J* = 6.3, 1.6 Hz, 1H, Ph, *p*-cym), 4.91 – 4.87 (m, 2H, cp), 4.85 (dd, *J* = 2.7, 1.4 Hz, 1H, cp) 4.76 (dq, *J* = 2.7, 1.3 Hz, 2H, cp), 4.72 (dq, *J* = 2.6, 1.3 Hz, 1H, cp), 4.69 (dt, *J* = 2.6, 1.3 Hz, 1H, cp), 4.66 (dt, *J* = 2.6, 1.3 Hz, 1H, cp), 4.64 – 4.61 (m, 2H, cp), 4.57 (dd, *J* = 4.4, 2.0 Hz, 1H, CH-α N), 4.54 (dd, *J* = 4.8, 1.5 Hz, 1H, CH-α N), 4.03 (td, *J* = 2.6, 1.4 Hz, 1H, cp), 4.01 – 3.98 (m, 2H, cp), 3.92 (t, *J* = 2.0 Hz, 2H, cp), 3.90 – 3.85 (m, 2H: 1H, cp + 1H, CH_2-α N), 3.76 (s, 3H, OMe), 3.74 (s, 3H, OMe), 3.73 – 3.63 (m, 2H, CH_2-α N), 2.64 (sept, *J* = 6.9 Hz, 2H, CH – *i*-pr, *p*-cym), 2.31 – 2.14 (m, 2H, CH_2-β *C* = *O*), 2.13 (d, *J* = 1.5 Hz, 3H, NCMe), 2.10 (d, *J* = 1.4 Hz, 3H, NCMe), 2.07 – 1.90 (m, 6H: 4H, CH_2-γ *C* = *O* + 2H, CH_2-β *C* = *O*), 1.88 (s, 3H, CH_3, *p*-cym), 1.86 (s, 3H, CH_3, *p*-cym), 1.19 – 1.11 (m, 12H, CH_3 – *i*-pr, p-cym); 1H of CH_2-α N was not found. However, the 2D-HSQC experiment showed that the signal is overlapped with the singlet signal of a OMe group at δ 3.73 ppm (See Figure S54) $^{13}C\{^1H\}$ NMR (75 MHz, $CDCl_3$) δ 172.8 (*C* = *O* ester), 172.7 (*C* = *O* ester), 168.1 (*C* = *O*

amide), 168.0 (*C* = *O* amide), 134.7 (unresolved dd, Ph – P), 133.3 (d, $J_{P,C}$ = 9.7 Hz, Ph – P), 132.6 (d, $J_{P,C}$ = 51.4 Hz, Ph – P, C_{ipso}), 132.5 (d, $J_{P,C}$ = 52.0 Hz, Ph – P, C_{ipso}), 131.8 (Ph – P), 131.1 (Ph – P), 131.0 (Ph – P), 128.4 (Ph – P), 128.3 (Ph – P), 128.2 (d, $J_{P,C}$ = 2.8 Hz, Ph – P), 128.0 (Ph – P), 126.9 (C – NCMe), 126.8 (C – NCMe), 114.1 (d, $J_{P,C}$ = 3.1 Hz, Ph, C_{ipso}, *p*-cym), 114.0 (d, $J_{P,C}$ = 2.8 Hz, Ph, C_{ipso}, *p*-cym), 101.1 (Ph, C_{ipso}, *p*-cym), 101.0 (Ph, C_{ipso}, *p*-cym), 90.9 (d, $J_{P,C}$ = 2.5 Hz, Ph, *p*-cym), 90.7 (unresolved d, Ph, *p*-cym), 89.6 (d, $J_{P,C}$ = 5.2 Hz, Ph, *p*-cym), 89.5 (Ph, *p*-cym), 89.3 (d, *J* = 5.0 Hz, Ph, *p*-cym), 88.8 (d, *J* = 3.1 Hz, Ph, *p*-cym), 88.5 (d, $J_{P,C}$ = 2.9 Hz, Ph, *p*-cym), 79.4 (d, $J_{P,C}$ = 44.3 Hz, C – P, cp), 78.8 (d, $J_{P,C}$ = 44.4 Hz, C – P, cp), 77.7 (C – CONH, cp), 75.6 (unresolved dd, cp), 75.2 (d, $J_{P,C}$ = 11.4 Hz, cp), 74.8 (d, $J_{P,C}$ = 13.1 Hz, cp), 74.5 (d, $J_{P,C}$ = 12.3 Hz, cp), 74.1 (cp), 73.3 (d, $J_{P,C}$ = 12.7 Hz, cp), 73.0 (d, $J_{P,C}$ = 7.7 Hz, cp), 72.9 (d, $J_{P,C}$ = 8.7 Hz, cp), 72.2 (cp), 71.7 (cp), 70.9 (cp), 60.2 (CH-α N), 60.1 (CH-α N), 52.2 (OMe) 52.1 (OMe), 48.5 (CH_2-α N) 48.4 (CH_2-α N), 31.0 (CH – *i*-pr, p-cym), 30.9 (CH – *i*-pr, p-cym), 28.6 (CH_2-β *C* = *O*), 28.6 (CH_2-β *C* = *O*), 25.5 (CH_2-γ *C* = *O*), 25.4 (CH_2-γ *C* = *O*), 22.6 (CH_3 – *i*-pr, p-cym), 22.5 (CH_3 – *i*-pr, p-cym), 21.3 (CH_3 – *i*-pr, p-cym), 21.2 (CH_3 – *i*-pr, p-cym), 18.0 (CH_3, *p*-cym), 17.9 (CH_3, *p*-cym), 3.7 (CH_3, NCMe), 3.7 (CH_3, NCMe).$^{31}P\{^1H\}$ NMR (121 MHz, $CDCl_3$) δ 28.7, 28.5. MS (ESI+): *m/z* 796 ($[M - NCMe - SbF_6]^+$).

2.7.4. Synthesis of cationic complex hexafluoroantimonate of [chloroacetonitril(p-cymene)(1-methylformylprolinate,1′-dicyclohexylphosphineferrocene)ruthenium (II)] ⟨RuCl(NCMe)(η^6-$C_{10}H_{14}$){PCy_2-[(η^5-C_5H_4)Fe(η^5-C_5H_4-Pro(OMe))]}⟩SbF_6 (7b'')

Complex (**7b''**). Starting from **6b''** (50 mg, 0.057 mmol) and $AgSbF_6$ (25.2 mg, 0.068 mmol) following the general procedure. **7b''** was isolated as an orange crystalline solid. Yield: 53 mg, 82 %. ^{1}H NMR (300 MHz, $CDCl_3$) δ 5.33 – 5.23 (m, 6H, Ph, *p*-cym), 5.04 (d, *J* = 6.4 Hz, 1H, Ph, *p*-cym), 5.00 (d, *J* = 6.1 Hz, 1H, Ph, *p*-cym), 4.96 – 4.91 (m, 2H, cp), 4.86 (br s, 1H, cp), 4.82 (br s, 2H, cp), 4.77 (br s, 3H, cp), 4.63 – 4.56 (m, 4H: 2H, CH-α *N* + 2H, cp), 4.55 – 4.51 (m, 2H, cp), 4.47 – 4.40 (m, 4H, cp), 3.95 – 3.81 (m, 2H, CH_2-α N), 3.78 (br s, 6H, OMe), 3.76 – 3.67 (m, 2H, CH_2-α N), 2.62 – 2.52 (m, 6H: 6H, Cy), 2.52 – 2.48 (m, 8H: 6H, NCMe + 2H, CH – *i*-pr, *p*-cym), 2.47 – 2.40 (m, 2H, Cy), 2.35 – 2.11 (m, 5H: 2H, CH_2-γ *C* = *O* + 2H CH_2-β *C* = *O* + 1H, Cy), 2.10 – 1.99 (m, 10H: 2H, CH_2-β *C* = *O* + 2H, CH_2-γ *C* = *O* + 6H, Cy), 1.95 (br s, 7H: 6H, CH_3, *p*-cym + 1H, Cy), 1.90 – 1.73 (m, 12H, Cy), 1.72 – 1.59 (m, 2H, Cy), 1.57 – 1.44 (m, 2H, Cy), 1.42 – 1.21 (m, 12H, Cy), 1.20 – 1.10 (m, 12H, CH_3 – *i*-pr, p-cym). $^{13}C\{^1H\}$ NMR (75 MHz, $CDCl_3$) δ 172.8 (*C* = *O* ester), 168.0 (*C* = *O* amide), 128.5 (C – NCMe), 128.4 (C – NCMe), 112.9 (Ph, C_{ipso}, *p*-cym), 112.5 (Ph, C_{ipso}, *p*-cym), 99.2 (Ph, C_{ipso}, *p*-cym), 99.1 (Ph, C_{ipso}, *p*-cym), 92.8 (d, $J_{P,C}$ = 5.8 Hz, Ph, *p*-cym), 90.0 (d, $J_{P,C}$ = 5.9 Hz, Ph, *p*-cym), 88.2 (d, $J_{P,C}$ = 7.3 Hz, Ph, *p*-cym), 86.1 (Ph, *p*-cym), 85.8 (d, $J_{P,C}$ = 4.3 Hz, Ph, *p*-cym), 80.4 (d, $J_{P,C}$ = 37.0 Hz, C – P, cp), 80.3 (d, $J_{P,C}$ = 36.5 Hz, C – P, cp), 77.8 (C – CONH, cp, partly overlapping with the solvent signal), 77.7 (C – CONH, cp, partly overlapping with the solvent signal), 74.0 (cp), 73.9 (cp), 73.8 (d, $J_{P,C}$ = 3.2 Hz, cp), 73.6 (d, $J_{P,C}$ = 2.9 Hz, cp), 73.5 (d, $J_{P,C}$ = 3.9 Hz, cp), 73.4 (d, $J_{P,C}$ = 5.0 Hz, cp), 73.1 (d, $J_{P,C}$ = 6.2 Hz, cp), 72.9 (d, $J_{P,C}$ = 4.6 Hz, cp), 72.8 (cp), 72.7 (cp), 72.4 (cp), 71.5 (cp), 71.0 (cp), 60.2 (CH-α N), 60.1 (CH-α N), 52.2 (OMe), 48.5 (CH_2-α N), 41.8 (d, $J_{P,C}$ = 13.1 Hz, CH- Cy), 41.5 (d, $J_{P,C}$ = 12.1 Hz, CH-Cy), 38.9 (unresolved dd, CH- Cy), 30.9 (CH – *i*-pr, p-cym), 29.9 (d, $J_{P,C}$ = 4.6 Hz, Cy), 29.8 (d, $J_{P,C}$ = 2.0 Hz, Cy), 29.7 (Cy), 29.3 (Cy), 28.6 (CH_2-β *C* = *O*), 27.9 (d, $J_{P,C}$ = 2.3 Hz, Cy), 27.7 (br s, Cy), 27.5 (d, $J_{P,C}$ = 2.5 Hz, Cy), 27.2 (Cy), 27.1 (Cy), 26.1 (Cy), 25.9 (Cy), 25.5 (CH_2-γ *C* = *O*), 22.7 (CH_3 – *i*-pr, p-cym), 22.6 (CH_3 – *i*-pr, p-cym), 21.6 (CH_3 – *i*-pr, p-cym), 17.9 (CH_3 – *p*-cym), 4.2 (CH_3 – NCMe). $^{31}P\{^1H\}$ NMR (121 MHz, $CDCl_3$) δ 26.7, 26.3. MS (ESI+): *m/z* 808 ($[M - NCMe - SbF_6]^+$).

2.8. X-ray crystal structure determination of compounds (S)-(η^5-C_5H_4-$PSeR_2$)Fe[η^5-C_5H_4-Pro(OMe)] [R= Ph (5a'^{,Se}); R= Cy (5b'^{,Se})]

Crystals suitable for single crystal X-ray diffraction analysis were grown from slow evaporation of ether (orange crystals for both compounds **5a''^{Se}** and **5b''^{Se}** were obtained). The crystal structures of **5a''^{Se}** and **5b''^{Se}** were determined by means of single crystal X-ray diffraction at room temperature. A complete dataset for each compound was acquired in a SMART-APEX II CCD diffractometer system. Data reduction was performed by using SAINT (M. SAINTPLUS V6.22 Bruker AXS Inc., WI, USA., in.). Multi-scan or face-indexed absorption corrections were applied using SADABS (W. Bruker AXS Inc. Madison, USA., SADABS, in, 2012). Structure solution by direct methods and completed by Difference Fourier Synthesis and refinement by least-squares using SHELXL [27] (G.M.S.N.V. Sheldrick, Bruker AXS Inc., Madison, WI, USA, 2000., in.). Hydrogen atoms positions were calculated after each cycle of refinement with SHELXL using a riding model for each structure, with C—H distance of 0.93 Å. U_{iso}(H) values were set equal to 1.2 U_{eq} of the parent carbon atom. During the last stages of the refinement of **5a''^{Se}**, it was clear that the dataset corresponds to an inversion twin. To address this, inversion twin refinement was performed with batch scale factor (BASF) of 0.03192. During the final stages of structural refinement of **5b''^{Se}**, it became evident that a solvent molecule occupied the intermolecular space. Despite our efforts to model it, we did not achieve a satisfactory model. At this juncture, we opted to use the SQUEEZE method, which is well-documented for modelling unresolved electron density, to account for the effect of the disordered solvent [28,29]. The absolute structure for each compound was reliably determined by using the Flack parameter ($[(I^+)-(I^-)]/[(I^+)+(I^-)]$ [30]. A summary of crystallographic and refinement details for both compounds is available as Supporting Information (Table S1).

CCDC **2414938** (**5a''^{Se}**) and CCDC **2415043** (**5b''^{Se}**) contain the supplementary crystallographic data for this paper. These data can be obtained free of charge from The Cambridge Crystallographic data Center *via* the link http://www.ccdc.cam.ac.uk/data_request/cif

2.9. Electrochemical measurements

The electrochemical measurements were performed on a CHI660 electrochemical workstation (CH Instruments) using a three-electrode system: platinum wire as the counter electrode, Ag/AgCl (saturated KCl) as the reference electrode, and Pt electrode with a geometric area of 0.03 cm^2 as the working electrode. All experiments were carried out under argon atmosphere at room temperature (ca. 20 °C) in a three-compartment, three-electrode anchor-type electrochemical cell setup. Samples were dissolved under argon atmosphere in anhydrous dichloromethane to give solutions containing 1 mM of the analyte and 0.1 M of tetrabutyl ammonium hexafluorophosphate ($TBAPF_6$) (99 %, Sigma-Aldrich). All electrochemical responses were measured at a scanning rate of 0.100 $V.s^{-1}$.

3. Results and discussion

3.1. Synthesis and characterization of the ligands 5a'–b''

The synthetic route employed for the synthesis of new ferrocenylphosphine-amino acid ligands (*s*)-(η^5-C_5H_4-PR_2)Fe(η^5-C_5H_4-AA) [*R*= Ph, Cy. AA= *l*-Glu(OMe)$_2$, l-Pro(OMe)] is shown in Scheme 1.

The synthesis starts with the reaction of precursor 1,1′-dibromoferrocene 2 with the corresponding chlorodiphosphine $ClPR_2$ [*R* = Ph (**3a**); Cy (**3b**)] as described by Butler and coworkers [24]. Compounds **3a** and **3b** were subsequently reacted with an excess of butyllithium and gaseous carbon dioxide (CO_2), as a variation of the previously reported procedure [22], to obtain the corresponding ferrocenylphosphine carboxylic acids **4a** and **4b** with good yields. Finally, the synthesis of the air-stable ferrocenylphosphine-amino acid ligands was achieved using a new methodology based on the procedure published by Metzler Nolte and coworkers [31], using protected proline or glutamic acid, mediated by o-Benzotriazol-1-yl-N,N,N',N'-tetramethyluronium tetrafluoroborate (TBTU) as a coupling reagent, NEt_3, and DMF as the solvent, leading to the respective ferrocenylphosphine-amino acid ligands **5a'–b''** as

orange solids in 71 % – 79 % yield after column chromatography purification. Ligands **5a'–b''** proved to be stable in solid state under aerobic conditions. However, in solution, ligands were prone to form the corresponding phosphine oxide. Ligand **5a'** was previously reported by Štěpnička and coworkers [20].

The compounds **5a'–b''** were characterized by multinuclear (^{1}H, ^{13}C{^{1}H}, ^{31}P{^{1}H} and 2D-HSQC for assignments) NMR spectroscopy and by high-resolution mass spectroscopy. NMR characterization of these compounds shows in the ^{1}H NMR spectra the expected signals associated with the CH groups of the ferrocene backbone between δ 4.81 and 4.08 ppm. For the **5a** family, the signals of the aromatic rings of the diphenylphosphine moiety were in the range of δ 7.60 – 7.30 ppm and, for the **5b** family, the signals for the cyclohexyl rings between δ 1.75 – 1.18 ppm. The amino acidic fragment shows the signals in the ^{1}H NMR spectra associated with the secondary amide hydrogen of the glutamic acid derivatives at δ 6.61 and 6.85 ppm, for ligands **5a'** and **5a''** respectively. The signal of the chiral α-hydrogen of the amino acid moiety is also present for the four ligands and ranged between δ 4.80 – 4.50 ppm as expected. Also, the four ligands show the signals of the methyl ester protecting groups around δ 3.70 ppm.

The ^{13}C{^{1}H} NMR spectra for all ligands show signals ranging from δ 173 – 172 ppm corresponding to an ester-type carbon atom, with the presence of signals between δ 171 – 168 ppm corresponding to an amide-type carbon atom. The carbonyl shift observed for the amide group in the compounds **5a'–b''** is the expected for *α,β*-unsaturated amides, where these amides exhibit an upfield shift of the signal due to the increase of the electronic density at the carbonyl carbon mediated by the delocalization of the olefinic *π*-electrons towards the carbonyl carbon [32]. This effect also decreases the electronic density at the olefinic carbon and generates a chemical shift to lower field of this signal, which is observed with the singlet signal of the quaternary cp-carbon bounded to the amide group between δ 76 – 75 ppm. These results confirm the coupling between the organometallic acids and the amino group of the protected amino acids.

The chemical shifts of the phosphorus nuclei in the ^{31}P{^{1}H} NMR for -PPh_2 and -PCy_2 groups are ranged in the expected zone (δ −17.8 ppm for **5a'** and δ −17.6 ppm for **5a''**; δ −8.8 ppm for **5b'** and δ −8.2 ppm for **5b''**). However, these signals show a slight displacement toward lower field when glutamic acid is replaced with proline.

3.2. Synthesis of the P-Selenides from 5a'–b'' and crystal structure of 5a''^{Se} and 5b''^{Se}

To confirm that the amino acid affects the electronic properties of the phosphine group, phosphine selenides were synthesized and studied by ^{31}P NMR [33,34]. The coupling constant $^{1}J_{P\text{-}Se}$ reflects the s character of the phosphorus lone pair based on the steric and electronic properties of the phosphine substituents. The selenides were obtained in quantitative yield upon the reaction of the corresponding ligand **5** with selenium black and isolated as air-stable orange solids (Scheme 2). The results in Table 1 summarize the coupling constant obtained for compounds **5a'^{Se}–b''^{Se}** and help to confirm the hypothesis that the amino acid has a significant effect on the basicity of the electronic pair of the phosphine. The $^{1}J_{P\text{-}Se}$ values are in the range of previously reported phosphine selenides of the commonly used triphenylphosphine ($SePPh_3$= 730 Hz) and bis-diphenylphosphineferrocene [Se(dppf)= 737 Hz], which indicates a basic character of the phosphine groups evaluated [33–35].

Table 1
Data of chemical shifts and coupling constants for the phosphine selenides.

Phosphine selenide	δ (^{31}P=Se) [ppm]	$^{1}J_{P\text{-}Se}$ (Hz)
5a'^{Se}	31.8	721.9
5a''^{Se}	31.3	735.0
5b'^{Se}	50.0	687.4
5b''^{Se}	49.5	700.5

Previous reports highlight that the inclusion of different groups to the opposite cp ring of the ferrocene moiety such as phosphine groups [36,37], carbonyl-phosphine groups [38], sulfonate groups [7], and substitution of the hydrogen atoms of the cp rings for more electro-donating groups [39,40], have little to no effect on the basicity of the primary phosphine group. However, in the case of the ligands with the glutamate moiety, the inclusion of this amino acid gives more basic phosphine groups than the ferrocenylphospine groups without modification [35,37], with coupling constant values similar to those reported for the ferrocenyl-carboxamide ligands $PPh_2FcCONHMe$ ($^{1}J_{P\text{-}Se}$= 718 Hz) and $PCy_2FcCONHMe$ ($^{1}J_{P\text{-}Se}$= 686 Hz) [41]. Comparing the ^{31}P{^{1}H} chemical shifts of the free ligands bearing the glutamate moiety and the $PR_2FcCONHMe$ ligands (δ −16.7 ppm for PPh_2 and δ −7.6 ppm for PCy_2) [41,42], this indicates that the contribution of the glutamate over the phosphine group comes from its electronic properties, since the glutamate induce a higher inductive effect over the phosphorus atom than the small methyl-amide fragment. This effect is also corroborated when comparing the ^{31}P{^{1}H} shift of the free ligands bearing the glutamate moiety and the effect generated by the electro-withdrawing group CN in the phosphino-cyanoferrocene ligands and their corresponding selenides [43,44].

Moreover, the structure of compounds **5a''^{Se}** and **5b''^{Se}** could be determined by single-crystal X-ray diffraction. The most representative bond distances and angles are collected in Table 2, while ORTEP-type views of the molecules are shown in Fig. 2.

Compounds **5a''^{Se}** and **5b''^{Se}** crystallize in the monoclinic crystal system ($P2_1$ space group), with one single molecule present in the asymmetric unit. For both molecules, the ferrocene fragment adopts its usual geometry, with Fe – C bond distances between 2.008(18) – 2.042 (19) Å for compound **5a''^{Se}** and 1.914(11) – 1.997(16) Å for compound **5b'^{Se}**, in addition to similar distances between the metal and each cp ring (Fe – Cg_1 and Fe – Cg_2). These values are according to the range reported in the literature for diphosphinoferrocene selenides containing amino acid fragments [41]. Moreover, the angle between the cp rings for both compounds is below 4°, which indicates that the compounds do not suffer distortion in the ferrocenyl fragment upon the addition of the corresponding phosphine and amino acid group. The dihedral angle τ showed that, for both compounds, the cp rings adopt an eclipsed anticlinal conformation (−153.42° for **5a''^{Se}**; −141.99° for **5b''^{Se}**).

In the amino acid group, the bond distance between the C_6 – C_{23} carbons, as well as between the *C* = *O* and N – C heteroatoms, indicate the correct formation of the amide group and its bond to the ferrocenyl fragment; the double bond character of the *C* = *O* group is observed,

Table 2
Selected geometric parameters for compounds 5a''^{Se} and 5b''^{Se}.

Parameters	5a''^{se}	5b''^{se}
Distance C – C cp (Å)	2.008(18) – 2.042(19)	1.914(11) – 1.997(16)
Distance Fe – Cg_1 (Å)	1.632	1.573
Distance Fe – Cg_2 (Å)	1.646	1.574
Cp_1 – Cp_2 (°)	1.26	3.59
τ (°)	−153.42	−141.99
C_6 – C_{23}	1.50(2)	1.412(18)
C = *O* (Å)	1.231(19)	1.165(15)
N – C_{23} (Å)	1.34(2)	1.320(16)
O = *C* – N (°)	119(2)	118(1)
C_{24} – N – C_{27} (°)	109(1)	116(1)
C_{23} – N – C_{27} (°)	119(1)	116(1)
φ_1 (°)	176(3)	179(2)
φ_2 (°)	174(2)	−180(2)
P – Se (Å)	2.100(5)	2.005(4)
P – C_{11}/C_{17} (Å)	1.798(17) / 1.820(19)	1.733(11) / 1.726(10)
PR_3 (°)	317.5	320.5

Cp_1= cp bonded to diphosphine group. Cp_2= cp bonded to amide group. Cg_1 and Cg_2 are the respective centroids. τ= dihedral angle C_1 – Cg_1 – Cg_2 – C_6. φ_1= dihedral angle between cp_2 and amide group; φ_2= dihedral angle between nitrogen and neighboring carbons. PR_3= Sum of the bond angles between the atoms bonded to the phosphrus atom.

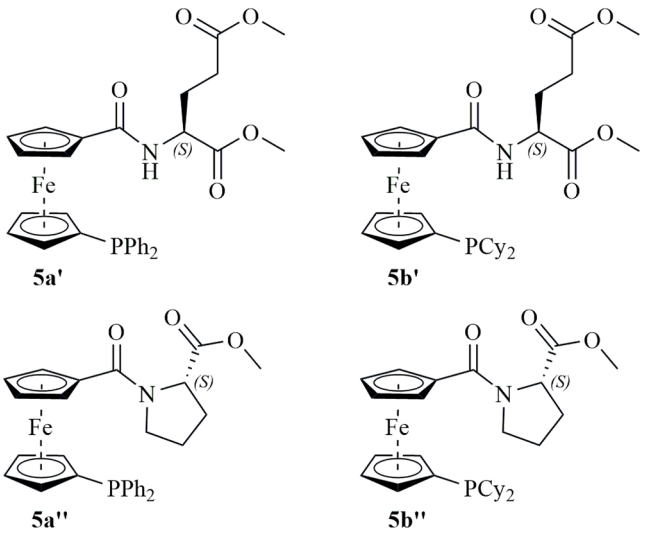


Fig. 1. Ferrocenylphosphine-amino acid ligands synthetized in this work.

with a shorter bond distance respect to N – C bond. These values are similar to those reported for ferrocenylcarboxamide-type compounds [45].

On the other hand, the bond angles of the amide group and the bond angles of the nitrogen respect to the neighboring carbons, together with the dihedral angles φ_1 and φ_2, indicate that the amide group adopts a trigonal geometry and a planar conformation with respect to the cp ring of the ferrocenyl fragment. In addition, the stereochemistry of the chiral carbon C_{27} is corroborated [*(S)* configuration], which is conserved unchanged from the amino acid precursor proline.

The integrity of the phosphine group for both compounds is corroborated by observing the values of the bond distances between P – C_1 and P – C_{11}/C_{17}, as well as the sum of the bond angles between the atoms bonded to the phosphorus atom (317.5° for **5a''^{Se}**, 320.5° for **5b''^{Se}**), are within the values reported in the literature for these phosphine groups [3,41,45–47]. The conformation of the R groups bonded to the phosphorus atom is also corroborated: planar conformation is observed for the phenyl groups of compound **5a''^{Se}** and chair conformation for the cyclohexyl groups of compound **5b''^{Se}**. The bond distances observed for the P – Se bonds are also within the value reported for both phosphine groups [48,49].

3.3. Synthesis of neutral and cationic ruthenium complexes from ligands 5a'–b''

Additionally, the coordinative properties of these new ligands were evaluated towards the coordination to a Ru(II) center. For these assays, 2 equivalents of ligands **5a'–b''** react with 1 equivalent of the complex $[Ru(p\text{-cymene})Cl_2]_2$ in dichloromethane (Scheme 3), giving deep red-colored four bimetallic complexes with excellent yields (81 – 97 %). Complex **6a'** was previously reported by Štěpnička and coworkers [20].

The ^{1H}NMR and $^{13}C\{^1H\}$ NMR spectra of these complexes show signals similar to the corresponding free ligands, in addition to those associated with the *p*-cymene ligand coordinated to the ruthenium center. Moreover, the coordination of the phosphorus atom was confirmed by the chemical shift displaced to lower field of the phosphorus signal in the $^{31}P\{^1H\}$ NMR spectra with respect to the free ligand. The complexes present signals between 16.5 – 19.0 ppm, according to literature reports [18,20,21,41,46]. The ESI+ mass spectra showed pseudomolecular ion $[M - Cl]^+$.

Removal of the chloride ligands from **6a'–b''** with 1 equivalent of the silver salt AgSbF in the presence of acetonitrile, complexes reacted to form three new air-stable cationic bimetallic complexes of ruthenium (Scheme 3). The complexes were isolated as orange crystalline solids with excellent yields (82 – 90 %). However, complex **7b'** could not be obtained in pure form and hence was not possible to be isolated. The ^1H NMR and $^{13}C\{^1H\}$ NMR spectra of the complexes **7a', 7a''** and **7b''** show duplicated signals, corresponding to the formation of 2 diastereomers for each complex: the ruthenium center becomes a stereocenter with the presence of 4 different ligands in the coordination sphere (Cl, NCMe, *p*-cym, PR_2) in addition of the chiral carbon present in the amino acid moiety of the phosphine ligand, resulting in a mixture of diastereomers (Fig. 3) [50–52].

These NMR signals are similar to the corresponding neutral complex, with a slightly displaced chemical shift to lower field due to the positive charged complex, in addition to those associated with the acetonitrile ligand coordinated to the ruthenium center. Additionally, a higher chemical shift displaced to lower field of the phosphorus signal in the $^{31}P\{^1H\}$ NMR spectra with respect to the neutral complex was observed, according to literature reports [19]. For complexes **7a''** and **7b''**, the $^{31}P\{^1H\}$ NMR showed some minor signals related to the coordination modes of the ligand in solution (discussed further below). The $^{31}P\{^1H\}$ NMR also showed a duplicated pattern of signals (Fig. 4).

The integration of the $^{31}P\{^1H\}$ NMR signals of the complexes showed an equal ratio for both enantiomers in the complex **7a'** (1:1 ratio) and a slightly predominance of one of the enantiomers in the complexes with the proline moiety **7a''** and **7b''** (53:47 ratio). The ESI+ mass spectra showed pseudomolecular ion $[M - NCMe - SbF_6]^+$.

3.4. Evaluation of the coordinative capacities of ligands 5a'–b''

To evaluate the bidentate coordinative capacity of ligands **5a'–b''** once coordinated to the ruthenium center, some tests were carried out by removal of the chloride ligand in the neutral complex **6a'** with the salt $AgSbF_6$ in dichloromethane. In the absence of a coordinative ligand, some signals of interest were observed in the experiment. The ^{31}P-NMR

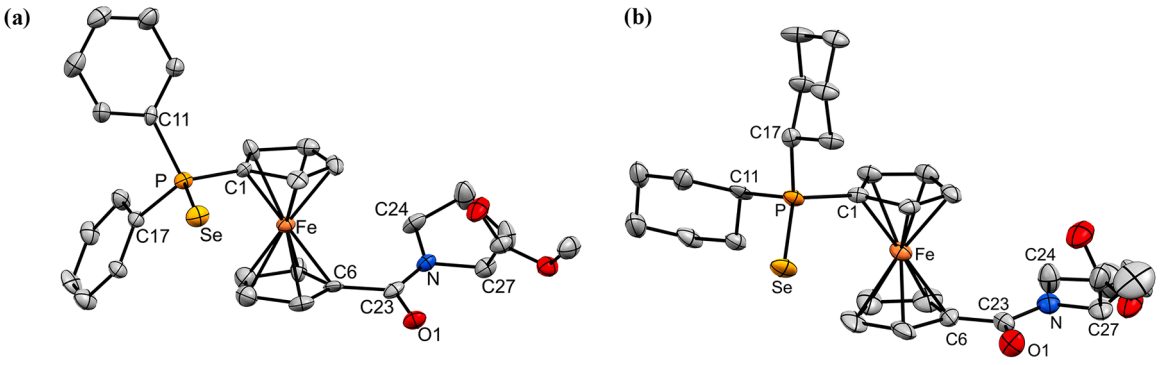


Fig. 2. ORTEP diagram of the crystal structure obtained for the compounds (a) **5a''^{Se}** and (b) **5b''^{Se}**. Gaussian ellipsoids for all non-hydrogen atoms are plotted at a 20 % probability level. Hydrogen atoms are omitted from the figure for clarity.

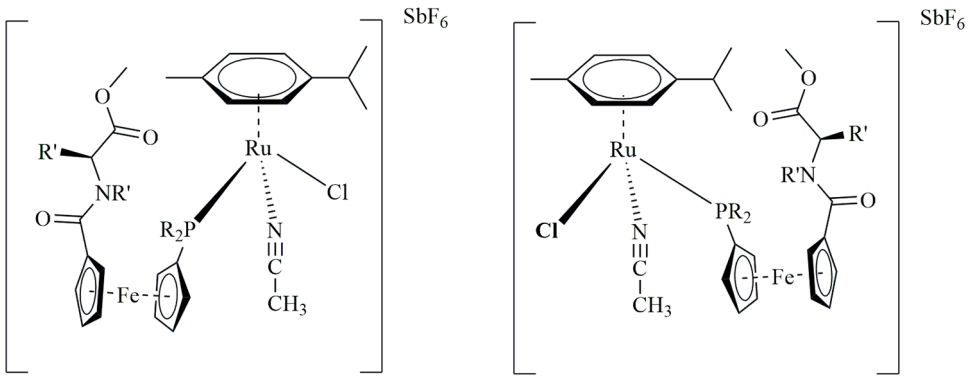


Fig. 3. Stereoisomers formed in the synthesis of the cationic complexes **7a'–b''**. *R*= Ph (**a**), Cy (**b**); R'= NH – CH_2CH_2COOMe (Glu) ('), N – $CH_2CH_2CH_2$ (Pro) ('').

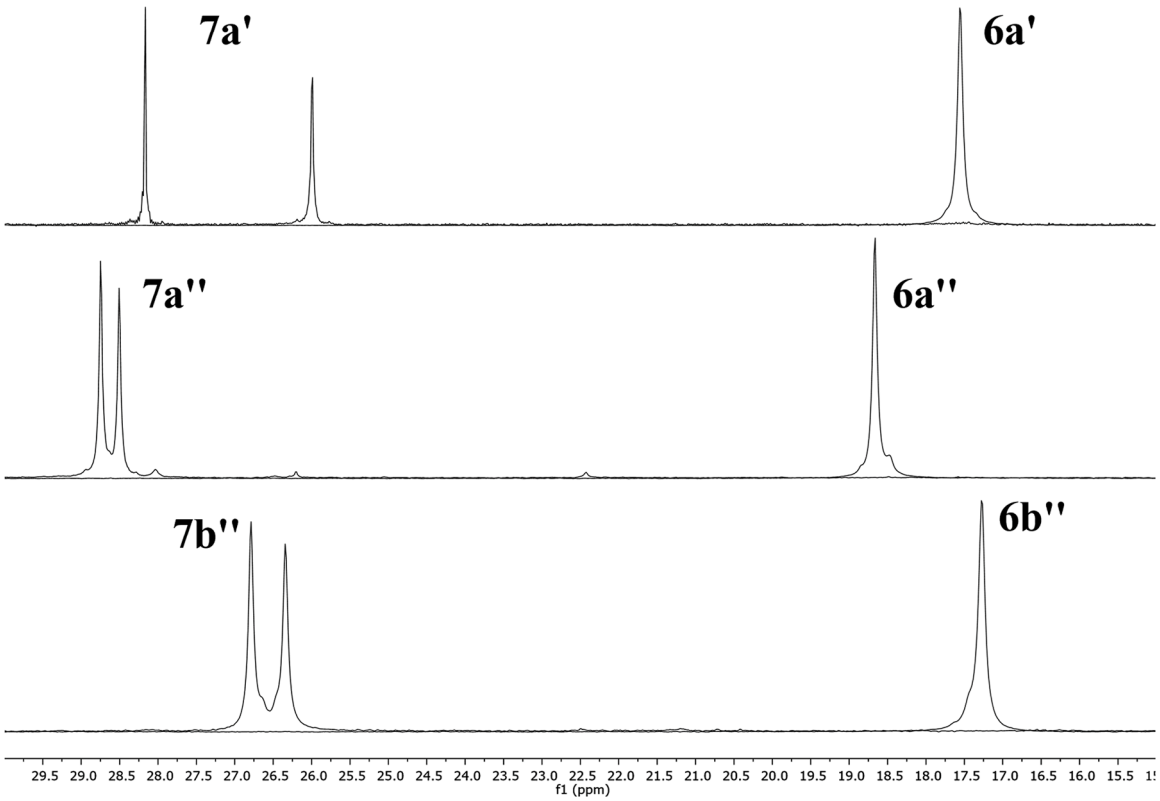


Fig. 4. $^{31}P\{^1H\}$ NMR Chemical shift displacements observed for cationic complexes **7a', 7a''** and **7b''**.

spectra of the reaction mixture (Fig. 5) showed, in addition to the signal of the phosphorus atom of the neutral complex **6a'**, signals corresponding to the formation of two different compounds in the reaction mixture, related to the coordination modes of the glutamic acid fragment to the metallic center (Scheme 4).

The doublet signal observed at δ 19.1 ppm is assigned to the formation of the cationic complex through the κ^2-P,O bidentate coordination of the ligand-mediated to the oxygen atom of the amide group. This coordination mode was observed by Bacchi and coworkers [53]. The doublet signals observed at δ 9.8 and δ 3.9 ppm (J_p= 51.4 Hz and 51.6 Hz, respectively) are assigned to the formation of the cationic complex through the κ^2-P,N bidentate coordination of the ligand trough to the lone pair of electrons of the nitrogen atom of the amide group, where the presence of 3 different substituents bonded to the nitrogen atom generate 2 different spatial arrangement, adopted by the substituents at the time of the coordination to the metal center, resulting in 2 separate signals in the spectra. These assignments are corroborated with the displacement to lower field of the signals observed in the ^{1H}NMR spectra (Supporting Information, Figure S60) corresponding to the methoxy groups from the amino acid moiety (δ 3.95 – 3.65 ppm) and the characteristic doublet from the proton of the amide group (δ 8.51 ppm). These signal patterns have been observed in the coordination of bidentate phosphine-nitrogen chiral compounds to ruthenium complexes by Hounjet and coworkers [18,54]. On the other hand, the singlet signals at δ 25.3 ppm and δ 17.6 ppm correspond to the unsaturated cationic ruthenium complex and the neutral starting material **6a'**, respectively [55]. However, none of these species could be isolated from the reaction crude due to the electronic and structural properties of the amide group and its coordination capability to the ruthenium center, where a stronger sigma interaction is needed between the carbonyl moiety and the metal center to generate stable bidentate coordination [56], or deprotonation of the nitrogen atom to form a formal sigma bond to the metal

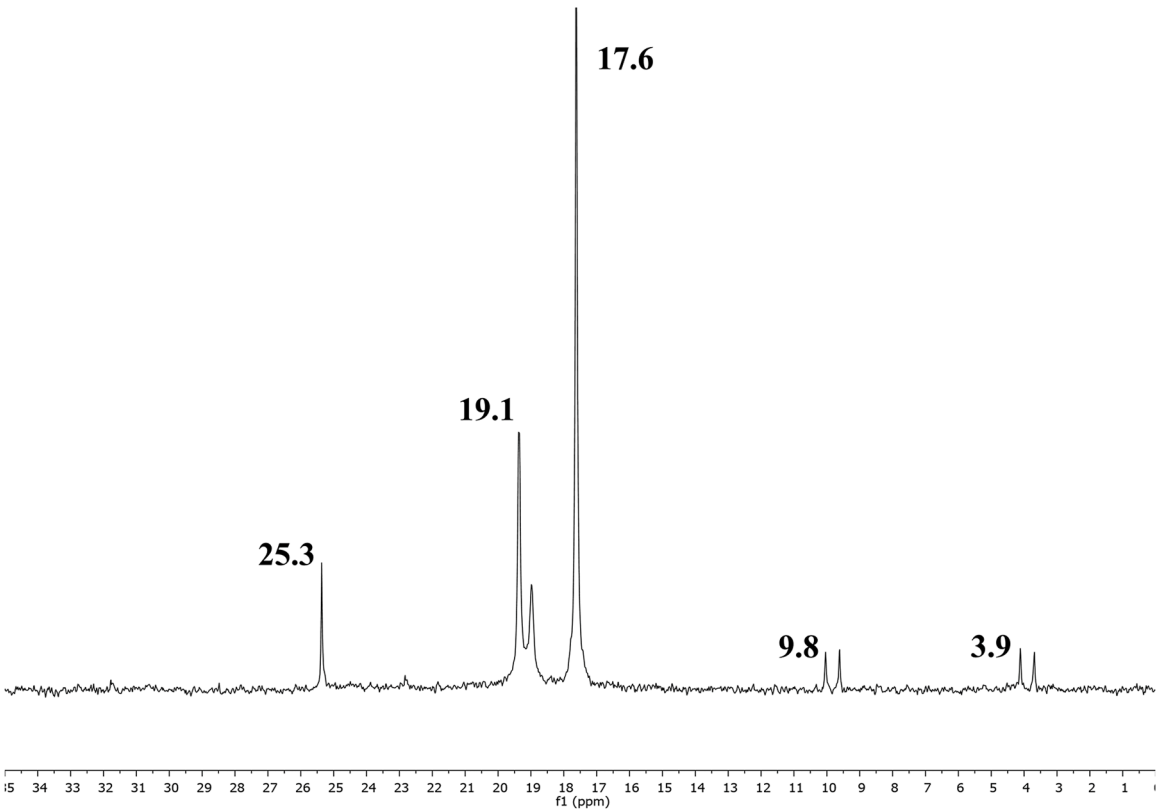


Fig. 5. ^{31}P-NMR spectra of the reaction mixture obtained upon reacting neutral complex **6a'** with a stoichiometric amount of $AgSbF_6$ in dichloromethane.

center.

Using two equivalents of the salt $AgSbF_6$ and neutral complex **6a''** under the same reaction conditions, some signals of interest were observed in the experiment. The ^{31}P-NMR spectra of the reaction crude (Fig. 6) showed the formation of three different complexes in the reaction mixture (Scheme 4): The doublet signal observed at δ 28.1 ppm, which corresponds to the formation of cationic complex **7a''**; a singlet observed at δ 33.6 ppm, assigned to the formation of the dicationic

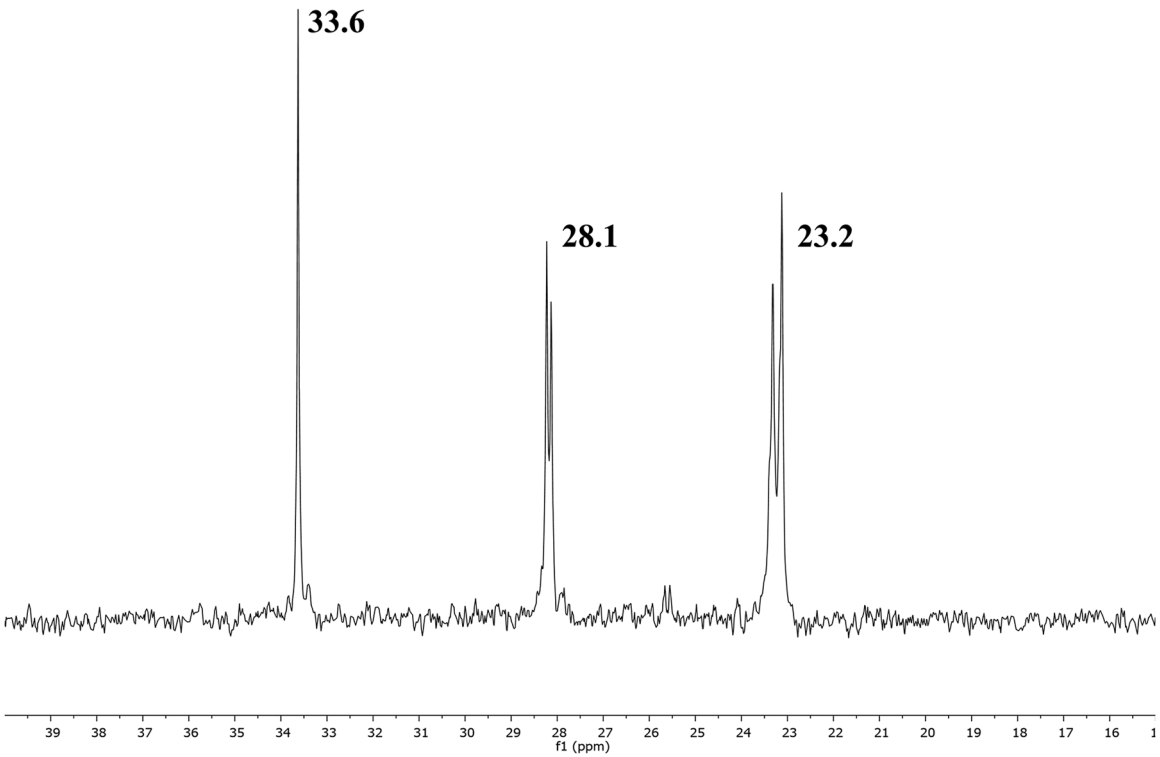


Fig. 6. ^{31}P-NMR spectra of the reaction mixture obtained upon reacting neutral complex **6a''** with 2 equivalents of $AgSbF_6$ in dichloromethane/acetonitrile.

complex with 2 acetonitrile ligands coordinated to the ruthenium center [19]; and a doublet signal at δ 23.2 ppm, assigned to the coordination κ^2-P,O of the ferrocenylphosphine-amino acid ligand through the oxygen atom of the amide group [53], with this specie being more prevalent than the rest of the complexes observed.

3.5. Electrochemical properties of ligands 5a'–b'' and bimetallic complexes 6a'–b'' and 7a', 7a'', 7b''

In order to determine a plausible electronic cooperative effect in the bimetallic compounds, electrochemical properties of free ligands **5a'–b''** and bimetallic complexes **6a'–b''** and **7a', 7a'', 7b''** were studied by cyclic voltammetry at a platinum disk electrode. Measurements were performed on anhydrous CH_2Cl_2 solutions containing 0.1 M $TBAPF_6$ as the supporting electrolyte and 1 mM of each of the compounds studied. All the measurements were counterbalanced with an internal ferrocene reference, but as there was no shift in this coupling, no correction of the exposed oxidation and reduction potential was necessary. Representative cyclic voltammograms are shown in Fig. 7, and the relevant data is summarized in Table 3.

The cyclic voltammograms (CV) of ligands **5a'–b''** showed a first oxidation and reduction peak between 0.91 – 0.60 V and 0.71 – 0.56 V, respectively, with a peak difference <200 mV measured at 100 mVs^{-1}, which is attributed to a one-electron redox changed centered on the ferrocene fragment of the ligands [$Fe^{(II/III)}$ couple] [57,58]. The difference between the oxidation and reduction peaks is greater than the reversibility criterion, and the ratio between the current peak intensities is not close to unity, thus the observed redox couple is considered quasi-reversible. It is also observed that the difference in oxidation and reduction peaks between ligands is associated with the electronic properties of the phosphine, where more electro-donating phosphine groups switch the observed peaks to less positive potentials [59].

For ligands **5a'** and **5b'**, when the switching potentials are increased, a second oxidation and reduction peak is observed at 200 mV more positive potentials than the first anodic peak observed (Supporting Information, Table S2). This second wave is attributed to the one-electron redox change centered on the ferrocene moiety [a second $Fe^{(II/III)}$ couple], but of the corresponding phosphine oxide formed from the oxidation of the phosphorus atom ($P^{III} \rightarrow P^{V}$) in the first anodic reaction. This species is generated in situ from an intramolecular electron transfer of the corresponding phosphine to the iron atom ($P^{III} \rightarrow Fe^{III}$) in the first anodic reaction (EC mechanism) [22,60–62]. Besides is not directly related to the phosphine group, this second wave is characteristic for each evaluated ligand. Switching to a more positive potential, no redox process was observed related to the amino acid fragment coupled to the ligands.

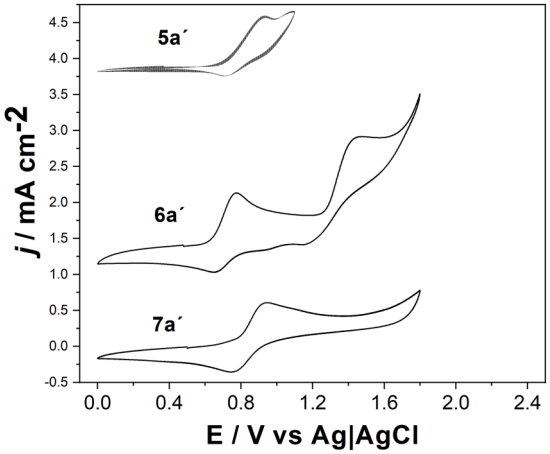


Fig. 7. Cyclic voltammograms of compounds **5–6–7a'**. Interphase: Pt + 1 mM of each compound and 0.1 M of $TBAPF_6$ in CH_2Cl_2, ν = 100 $mV.s^{-1}$, 1 cycle.

Table 3
Summary of electrochemical data for free ligands 5a'–b'' and bimetallic complexes 6a'–b'' and 7a', 7a'', 7b''[a].

Comp.	E / V Fe (II/III)				E / V Ru (II/III)			
	$E^{\circ'}$	P_{ox}	P_{red}	ΔE_p	$E^{\circ'}$	P_{ox}	P_{red}	ΔE_p
5a'	0.81	0.91	0.71	0.20	-	-	-	-
5b'	0.65	0.70	0.59	0.11	-	-	-	-
5a''	0.69	0.73	0.64	0.09	-	-	-	-
5b''	0.60	0.63	0.56	0.07	-	-	-	-
6a'	0.71	0.76	0.66	0.10	1.29	1.41	1.17	0.24
6b''[b]	0.99	1.37	0.62	0.75	n.o.	n.o.	n.o.	n.o.
6a''	0.66	0.77	0.54	0.23	1.28	1.37	1.19	0.18
6b''	0.57	0.88	0.26	0.62	1.07	1.40	0.75	0.65
7a'	0.83	0.94	0.71	0.23	n.o.	n.o.	n.o.	n.o.
7a''	0.80	0.88	0.71	0.17	n.o.	n.o.	n.o.	n.o.
7b''	0.97	1.13	0.80	0.33	n.o.	n.o.	n.o.	n.o.

[a] See text for discussion. $E^{\circ'} = \frac{1}{2}(P_{ox} + P_{red})$. P_{ox} = oxidation peak, P_{red} = reduction peak; ΔE_p = peak difference. n.o.= not observed. [b]Poorly resolved wave.

On the other hand, for ligands **5a''** and **5b''**, the oxidation and reduction peaks of the second wave are observed at 120 mV more positive potentials than the $Fe^{(II/III)}$ couple and are partly overlapped with this couple. For ligand **5a''**, switching to more positive potentials, an irreversible oxidation peak is observed at 1.1 V, attributed to the one-electron oxidation of the carboxamide group [63]. However, for compound **5b''**, both second wave and carboxamide couples overlap with the first $Fe^{(II/III)}$ couple, which generates a poorly resolved single wave graphic, indicating an electronic coupling between the oxidizing centers of the ligand (Fe and P atoms) [63], and subsequent decomposition of the ligand by the oxidation of the carboxamide group. The electrochemical responses observed for the **5a'–b''** ligands are consistent with those reported for ferrocenylphosphino-carboxamide-type ligands [18, 20].

Cyclic Voltammograms for complexes **6a', 6a''**, and **6b''** showed the presence of two characteristic redox couples. The first redox couple, observed at lower oxidation potentials, is attributed to the $Fe^{(II/III)}$ couple related to the ferrocenylphosphine-amino acid ligands coordinated to the metal center, meanwhile, the second redox couple, at higher potentials, is attributed to the $Ru^{(II/III)}$ couple. The second wave observed in the free ligands corresponding to the $Fe^{(II/III)}$ couple of the phosphine oxide is not observed in the CV due to the unavailability of the lone electron pair of the phosphorus atom, which is used upon coordination to the ruthenium center.

The electron density loss on the phosphine group has a generalized influence on the ferrocene fragment, observed in the increase towards more positive oxidation potentials of the $Fe^{(II/III)}$ couple respect to the uncoordinated ligand, as well as the absence of the oxidation peak of the carboxamide group. However, for compound **6b'** it was not observed the $Fe^{(II/III)}$ couple of the ligand **5b'** due to an overlapping of the redox couples of both metal centers of the complex. This overlap is related to the σ-donor capability of ligand **5b'**, where an incremental of the electron density in the ruthenium center upon ligand coordination, compared to the other less-basic ligands, generates a decrease in the oxidation potential of the ruthenium [57,64,65], resulting in an electronic coupling between both metal centers. The ΔEp of the $Fe^{(II/III)}$ and $Ru^{(II/III)}$ couples for **6b'** and **6b''** are at least four times higher than those observed for **6a'** and **6a''**, which indicates an irreversible oxidation of the couples and probably decomposition of the compound in the process. For complex **6a'** and **6a''**, they exhibit ΔEp and current intensities values that classify them as quasi-reversible couples.

Substitution of the anionic chloride ligand by the neutral acetonitrile ligand produces positively charged complexes, which results in more difficult species to oxidize. This is observed in the positive shift of the corresponding $Fe^{(II/III)}$ couple of each cationic complex **7a', 7a'', 7b''** as

compared with the corresponding neutral complex **6a', 6a'', 6b''**. Electrochemical responses for cationic complexes showed only one quasi-reversible couple, attributable to the $Fe^{(II/III)}$ couple. The $Ru^{(II/III)}$ couple is shifted to an even more positive potential, disappearing in the working windows optimized for this process, indicating a non-electronic coupling between metals in the cationic complexes. The electrochemical responses observed for the bimetallic ruthenium complexes are consistent with those reported in the literature [19,20].

4. Conclusions

In summary, we presented the synthesis of new ferrocenylphosphine-amino acid ligands through a facile and economic synthetic route, coupling diphosphineferrocenecarboxylic acids with amino acids methyl protected fragments and TBTU within excellent yields. The electronic effect of the amino acid moiety over the phosphine groups was demonstrated for the first time through the synthesis of the phosphine selenides of the ligands **5a'–b''**, characterizing complexes **5a''^{Se}** and **5b''^{Se}** by single-crystal X-ray diffraction techniques. The coordination capabilities of the synthesized ligands were also evaluated, resulting in four neutral ruthenium complexes and three cationic ruthenium complexes. All the synthesized compounds were characterized electrochemically and by NMR spectroscopy. Further studies aiming at exploring the catalytic capabilities of the synthesized complexes in the asymmetric transfer hydrogenation, as well the coordination of these ferrocenylphosphine-amino acid ligands in other metal centers are in progress in our laboratories and will be a subject of future contribution.

CRediT authorship contribution statement

Andrés Terán: Writing – original draft, Investigation, Formal analysis. **Loreto Hernández:** Writing – original draft, Investigation, Formal analysis. **Andrés Vega:** Writing – original draft, Formal analysis. **Diego Sierra:** Writing – review & editing, Writing – original draft, Supervision, Investigation.

Declaration of competing interest

The authors declare that they have no known competing about financial interests or personal relationships that could have appeared to influence the work reported in this paper.

Acknowledgments

A. Terán acknowledges Agencia Nacional de Investigación y Desarrollo ANID (Beca de Doctorado Nacional, File 21210985), Programa Conjunto de Doctorado en Ciencias mención Química, Universidad de Valparaíso-Universidad Técnica Federico Santa María, and Dirección de Postgrado y Programas - Universidad Técnica Federico Santa María. A. Terán and D. Sierra acknowledge J. García-Álvarez and A. Presa Soto from Laboratorio de Química Sintética Sostenible (*QuimSinSos*) for their cooperation and support in this investigation.

Supplementary materials

Supplementary material associated with this article can be found, in the online version, at doi:10.1016/j.jorganchem.2025.123829.

Appendix A. Supplementary data

Spectroscopy data and Cyclic Voltammograms of synthetized compounds, Table S2 with the electrochemical data observed for ligands **5a'-b''**, Table S1 with crystallographic and refinement details, alternative views of the molecular structures **5a''^{Se}** and **5b''^{Se}** with full atom labelling are provided as a PDF file in the supplementary materials.

Data availability

Data will be made available on request.

References

[1] C. Chen, T.M.J. Anselment, R. Fröhlich, B. Rieger, G. Kehr, G. Erker, O-diarylphosphinoferrocene sulfonate palladium systems for nonalternating ethene-carbon monoxide copolymerization, Organometallics 30 (2011) 5248–5257, https://doi.org/10.1021/om200628r.

[2] K. Jess, D. Baabe, T. Bannenberg, K. Brandhorst, M. Freytag, P.G. Jones, M. Tamm, Ni-Fe and Pd-Fe interactions in nickel(II) and palladium(II) complexes of a ferrocene-bridged bis(imidazolin-2-imine) ligand, Inorg Chem 54 (2015) 12032–12045, https://doi.org/10.1021/acs.inorgchem.5b02457.

[3] H. Charvátová, T. Vašíček, I. Císařová, P. Štěpnička, Synthesis and structural characterization of ferrocene phosphines modified with polar pendants and their palladium(II) complexes. Part II: n-aminocarbonyl and N-acyl phosphinoferrocene carbohydrazides, J Organomet Chem 861 (2018) 207–218, https://doi.org/10.1016/j.jorganchem.2018.02.044.

[4] D.Y. Huang, Q.J. Yao, S. Zhang, X.T. Xu, K. Zhang, B.F. Shi, Amide-directed cobalt (III)-catalyzed C-H amidation of ferrocenes, Org Lett 21 (2019) 951–954, https://doi.org/10.1021/acs.orglett.8b03938.

[5] D. Sierra, C. Contreras, J. Francos, J. Gómez, V. Cadierno, Novel ferrocenylphosphino sulfonates: synthesis, crystal structure and preliminary application as ligands in aqueous catalysis, J Organomet Chem 854 (2018) 106–112, https://doi.org/10.1016/j.jorganchem.2017.11.019.

[6] J. Francos, M.E. Moreno-Narváez, V. Cadierno, D. Sierra, K. Ariz, J. Gómez, Gold(I) complexes with ferrocenylphosphino sulfonate ligands: synthesis and application in the catalytic addition of carboxylic acids to internal alkynes in water, Catalysts 9 (2019), https://doi.org/10.3390/catal9110955.

[7] M. Zábranský, I. Císařová, P. Štěpnička, Synthesis, coordination, and catalytic use of 1′-(Diphenylphosphino)ferrocene-1-sulfonate anion, Organometallics 37 (2018) 1615–1626, https://doi.org/10.1021/acs.organomet.8b00178.

[8] H. Charvátová, I. Císařová, P. Štěpnička, Synthesis of phosphanylferrocenecarboxamides bearing guanidinium substituents and their application in the palladium-catalyzed cross-coupling of boronic acids with acyl chlorides, Eur J Inorg Chem 2017 (2017) 288–296, https://doi.org/10.1002/ejic.201600461.

[9] P. Vosáhlo, L. Radal, M. Labonde, I. Císařová, J. Roger, N. Pirio, J.C. Hierso, P. Štěpnička, Synthesis and catalytic use of polar phosphinoferrocene amidosulfonates bearing bulky substituents at the ferrocene backbone, Organometallics 40 (2021) 1934–1944, https://doi.org/10.1021/acs.organomet.1c00244.

[10] W. Wu, S. Liu, M. Duan, X. Tan, C. Chen, Y. Xie, Y. Lan, X.Q. Dong, X. Zhang, Iridium catalysts with f-amphox ligands: asymmetric hydrogenation of simple ketones, Org Lett 18 (2016) 2938–2941, https://doi.org/10.1021/acs.orglett.6b01290.

[11] F. Ling, S. Nian, J. Chen, W. Luo, Z. Wang, Y. Lv, W. Zhong, Development of ferrocene-based diamine-phosphine-sulfonamide ligands for iridium-catalyzed asymmetric hydrogenation of ketones, Journal of Organic Chemistry 83 (2018) 10749–10761, https://doi.org/10.1021/acs.joc.8b01276.

[12] S. Nian, F. Ling, J. Chen, Z. Wang, H. Shen, X. Yi, Y.F. Yang, Y. She, W. Zhong, Highly enantioselective hydrogenation of non- ortho-substituted 2-pyridyl aryl ketones via iridium- f-diaphos catalysis, Org Lett 21 (2019) 5392–5396, https://doi.org/10.1021/acs.orglett.9b01415.

[13] J. Yu, J. Long, Y. Yang, W. Wu, P. Xue, L.W. Chung, X.Q. Dong, X. Zhang, Iridium-catalyzed asymmetric hydrogenation of ketones with accessible and modular ferrocene-based amino-phosphine acid (f-Ampha) ligands, Org Lett 19 (2017) 690–693, https://doi.org/10.1021/acs.orglett.6b03862.

[14] X. Tan, W. Zeng, J. Wen, X. Zhang, Iridium-catalyzed asymmetric hydrogenation of α-fluoro ketones via a dynamic kinetic resolution strategy, Org Lett 22 (2020) 7230–7233, https://doi.org/10.1021/acs.orglett.0c02565.

[15] G. Liu, C. Yin, X. Yang, A. Li, M. Wang, X. Zhang, X.Q. Dong, Highly chemo- and enantioselective Rh-catalyzed hydrogenation of β-sulfonyl-α,β-unsaturated ketones: access to chiral γ-ketosulfones, Org Lett 23 (2021) 19–24, https://doi.org/10.1021/acs.orglett.0c03517.

[16] J. Tauchman, I. Císařová, P. Štěpnička, Phosphinoferrocenyl carboxamides bearing glycine pendant groups: synthesis, palladium(II) complexes, and catalytic use in polar and aqueous reaction Media, Organometallics 28 (2009) 3288–3302, https://doi.org/10.1021/om900209j.

[17] J. Tauchman, I. Císařová, P. Štěpnička, Chiral phosphanylferrocenecarboxamides with amino acid pendant groups as ligands for Cu-mediated asymmetric conjugate additions of diethylzinc to chalcones - structural characterisation of precursors to the Cu catalyst, European J Org Chem (2010) 4276–4287, https://doi.org/10.1002/ejoc.201000480.

[18] J. Tauchman, I. Císaová, P. Štěpnička, Chiral phosphinoferrocene carboxamides with amino acid substituents as ligands for Pd-catalysed asymmetric allylic substitutions. Synthesis and structural characterisation of catalytically relevant Pd complexes, Dalton Transactions 40 (2011) 11748–11757, https://doi.org/10.1039/c1dt11230a.

[19] J. Tauchman, B. Therrien, G. Süss-Fink, P. Štěpnička, Heterodinuclear arene ruthenium complexes containing a glycine-derived phosphinoferrocene carboxamide: synthesis, molecular structure, electrochemistry, and catalytic

oxidation activity in aqueous media, Organometallics 31 (2012) 3985–3994, https://doi.org/10.1021/om3002087.
[20] J. Tauchman, G. Süss-Fink, P. Štěpnička, O. Zava, P.J. Dyson, Arene ruthenium complexes with phosphinoferrocene amino acid conjugates: synthesis, characterization and cytotoxicity, J Organomet Chem 723 (2013) 233–238, https://doi.org/10.1016/j.jorganchem.2012.10.009.
[21] J. Schulz, J. Tauchman, I. Císařová, T. Riedel, P.J. Dyson, P. Štěpnička, Synthesis, structural characterization and cytotoxicity of bimetallic chlorogold(I) phosphine complexes employing functionalized phosphinoferrocene carboxamides, J Organomet Chem 751 (2014) 604–609, https://doi.org/10.1016/j.jorganchem.2013.07.014.
[22] J. Podlaha, P. Štěpnička, J. Ludvík, I. Císařová, 1′-(diphenylphosphino) ferrocenecarboxylic acid and its P-oxide and methyl ester: synthesis, characterization, crystal structure, and electrochemistry, Organometallics 15 (1996) 543–550, https://doi.org/10.1021/om950528q.
[23] A. Shafir, M.P. Power, G.D. Whitener, J. Arnold, Inorganic syntheses. https://www.wiley.com/en-pk/Inorganic+Syntheses%2C+Volume+36-p-9781118744994, 2014 (accessed June 20, 2023).
[24] I.R. Butler, R.L. Davies, A rapid convenient synthesis of ferrocene-based triphos analogue ligands, Synthesis (Stuttg) 1996 (1996) 1350–1354, https://doi.org/10.1055/s-1996-4394.
[25] M.A. Bennett, T.N. Huang, T.W. Matheson, A.K. Smith, S. Ittel, W. Nickerson, 16. (η 6 -Hexamethylbenzene)Ruthenium complexes. Synth. React. Inorg. Metalorg, Chem, 1982, pp. 74–78, https://doi.org/10.1002/9780470132524.ch16.
[26] P. Štěpnička, I. Císařová, Selective borane reduction of phosphinoferrocene carbaldehydes to phosphinoalcohol-borane adducts. The coordination behaviour of 1-(diphenylphosphino)- 1′-(methoxymethyl)ferrocene, a new ferrocene O,P-hybrid donor prepared from such an adduct, Dalton Transactions 42 (2013) 3373–3389, https://doi.org/10.1039/c2dt32511j.
[27] G.M. Sheldrick, A short history of *SHELX*, Acta Crystallogr A 64 (2008) 112–122, https://doi.org/10.1107/S0108767307043930.
[28] A.L. Spek, *PLATON* SQUEEZE: a tool for the calculation of the disordered solvent contribution to the calculated structure factors, Acta Crystallogr C Struct Chem 71 (2015) 9–18, https://doi.org/10.1107/S2053229614024929.
[29] P. van der Sluis, A.L. Spek, BYPASS: an effective method for the refinement of crystal structures containing disordered solvent regions, Acta Crystallogr A 46 (1990) 194–201, https://doi.org/10.1107/S0108767389011189.
[30] S. Parsons, H.D. Flack, T. Wagner, Use of intensity quotients and differences in absolute structure refinement, Acta Crystallogr B Struct Sci Cryst Eng Mater 69 (2013) 249–259, https://doi.org/10.1107/S2052519213010014.
[31] D.R. Van Staveren, T. Weyhermüller, N. Metzler-Nolte, Organometallic β-turn mimetics. A structural and spectroscopic study of inter-strand hydrogen bonding in ferrocene and cobaltocenium conjugates of amino acids and dipeptides, Dalton Transactions (2003) 210–220, https://doi.org/10.1039/b208363a.
[32] M.U. Hasan, ^{13}C NMR spectra of some amides and imides. Effect of inductive and mesomeric interactions, cyclization and hydrogen bonding on ^{13}C NMR chemical shifts, Organic Magnetic Resonance 14 (1980) 447–450, https://doi.org/10.1002/mrc.1270140605.
[33] C.A. Tolman, Steric effects of phosphorus ligands in organometallic chemistry and homogeneous catalysis, Chem Rev 77 (1977) 313–348, https://doi.org/10.1021/cr60307a002.
[34] D.W. Allen, B.F. Taylor, The chemistry of heteroarylphosphorus compounds. Part 15. Phosphorus-31 nuclear magnetic resonance studies of the donor properties of heteroarylphosphines towards selenium and platinum(II), Journal of the Chemical Society, Dalton Transactions (1982) 51–54, https://doi.org/10.1039/DT9820000051.
[35] M.N. Chevykalova, L.F. Manzhukova, N.V. Artemova, Y.N. Luzikov, I.E. Nifantʹev, E.E. Nifantʹev, Electronndonating ability of triarylphosphines and related compounds studied by 31 P NMR spectroscopy, 2003.
[36] P. Vosáhlo, I. Císařová, P. Štěpnička, Comparing the asymmetric dppf-type ligands with their semi-homologous counterparts, J Organomet Chem 860 (2018) 14–29, https://doi.org/10.1016/j.jorganchem.2018.01.009.
[37] S.L. Kahn, M.K. Breheney, S.L. Martinak, S.M. Fosbenner, A.R. Seibert, W.S. Kassel, W.G. Dougherty, C. Nataro, Synthesis, characterization, and electrochemistry of compounds containing 1-diphenylphosphino-1 -(di-tert-butylphosphino)ferrocene (dppdtbpf), Organometallics 28 (2009) 2119–2126, https://doi.org/10.1021/om800850c.
[38] P. Vosáhlo, I. Císařová, P. Štěpnička, Synthesis, coordination behavior, and catalytic properties of dppf congeners with an inserted carbonyl moiety, New Journal of Chemistry 46 (2022) 21536–21552, https://doi.org/10.1039/d2nj04270c.
[39] J. Roger, S. Royer, H. Cattey, A. Savateev, R.V. Smaliy, A.N. Kostyuk, J.C. Hierso, Diastereoselective synthesis of dialkylated bis(phosphino)ferrocenes: their use in promoting silver-mediated nucleophilic fluorination of chloroquinolines, Eur J Inorg Chem 2017 (2017) 330–339, https://doi.org/10.1002/ejic.201600502.
[40] L. Radal, P. Vosáhlo, J. Roger, H. Cattey, R. Amardeil, I. Císařová, P. Štěpnička, N. Pirio, J.C. Hierso, Highly functionalized Brønsted Acidic/Lewis basic hybrid ferrocene ligands: synthesis and coordination chemistry, Eur J Inorg Chem 2019 (2019) 865–874, https://doi.org/10.1002/ejic.201801378.
[41] J. Schulz, P. Vosáhlo, F. Uhlík, I. Císařová, P. Štěpnička, Probing the influence of phosphine substituents on the donor and catalytic properties of phosphinoferrocene carboxamides: a combined experimental and theoretical study, Organometallics 36 (2017) 1828–1841, https://doi.org/10.1021/acs.organomet.7b00181.
[42] T.A. Fernandes, H. Solařová, I. Císařová, F. Uhlík, M. Štícha, P. Štěpnička, Synthesis of phosphinoferrocene amides and thioamides from carbamoyl chlorides and the structural chemistry of group 11 metal complexes with these mixed-donor ligands, Dalton Transactions 44 (2015) 3092–3108, https://doi.org/10.1039/c4dt03279a.
[43] K. Škoch, I. Císařová, Štěpnička, 1′-(diphenylphosphino)-1-cyanoferrocene: a simple ligand with complicated coordination behavior toward copper(I), Inorg Chem 53 (2014) 568–577, https://doi.org/10.1021/ic4026848.
[44] O. Bárta, I. Císařová, J. Schulz, P. Štěpnička, Assessing the influence of phosphine substituents on the catalytic properties of self-stabilised digold(<scp>i</scp>) complexes with supporting ferrocene phosphinonitrile ligands, New Journal of Chemistry 43 (2019) 11258–11262, https://doi.org/10.1039/C9NJ02555C.
[45] P. Štěpnička, B. Schneiderová, J. Schulz, I. Císařová, Synthesis, coordination properties, and catalytic use of phosphinoferrocene carboxamides bearing donor-functionalized amide substituents, Organometallics 32 (2013) 5754–5765, https://doi.org/10.1021/om400282z.
[46] J. Schulz, F. Horký, I. Císařová, P. Štěpnička, Synthesis, structural characterization and catalytic evaluation of anionic phosphinoferrocene amidosulfonate ligands, Catalysts 7 (2017), https://doi.org/10.3390/catal7060167.
[47] P. Vosáhlo, J. Schulz, K. Škoch, I. Císařová, P. Štěpnička, Synthesis and characterisation of palladium(ii) complexes with hybrid phosphinoferrocene ligands bearing additional O-donor substituents, New Journal of Chemistry 43 (2019) 4463–4470, https://doi.org/10.1039/c9nj00298g.
[48] K.D. Reichl, C.L. Mandell, O.D. Henn, W.G. Dougherty, W. Scott Kassel, C. Nataro, Synthesis and electrochemistry of 1,1′-bis(phosphino)cobaltocenium compounds, J Organomet Chem 696 (2011) 3882–3894, https://doi.org/10.1016/j.jorganchem.2011.09.004.
[49] G. Pilloni, B. Longato, G. Bandoli, B. Corain, Bonding ability of 1,1-bis(diphenylthiophosphoryl)ferrocene (dptpf) and its selenium analogue towards copper(I). Crystal structure of [Cu(dptpf)]BF 4, 1997.
[50] H. Brunner, Optical activity from asymmetric transition metal atoms, Angewandte Chemie International Edition in English 10 (1971) 249–260, https://doi.org/10.1002/anie.197102491.
[51] K. Mislow, J. Siegel, Stereoisomerism and local chirality, J Am Chem Soc 106 (1984) 3319–3328, https://doi.org/10.1021/ja00323a043.
[52] J.H. Nelson, Characterization of diastereomers by 31P{'H}, NMR spectroscopy (1995).
[53] A. Bacchi, P. Pelagatti, C. Pelizzi, D. Rogolino, Diastereomeric half-sandwich Ru(II) cationic complexes containing amino amide ligands. Synthesis, solution properties, crystal structure and catalytic activity in transfer hydrogenation of acetophenone, J Organomet Chem 694 (2009) 3200–3211, https://doi.org/10.1016/j.jorganchem.2009.05.010.
[54] L.J. Hounjet, M. Bierenstiel, M.J. Ferguson, R. McDonald, M. Cowie, Coordinatively diverse ortho -phosphinoaniline complexes of ruthenium and isolation of a putative intermediate in ketone transfer hydrogenation catalysis, Inorg Chem 49 (2010) 4288–4300, https://doi.org/10.1021/ic100165t.
[55] H. Aneetha, M. Jiménez-Tenorio, M. Carmen Puerta, P. Valerga, V.N. Sapunov, R. Schmid, K. Kirchner, K. Mereiter, Coordinatively unsaturated ruthenium phosphine half-sandwich complexes: correlations to structure and reactivity, Organometallics 21 (2002) 5334–5346, https://doi.org/10.1021/om020359r.
[56] H. Sigel, R.B. Martin, Coordinating properties of the amide bond. Stability and structure of metal ion complexes of peptides and related ligands, Chem Rev 82 (1982) 385–426, https://doi.org/10.1021/cr00050a003.
[57] P. Štěpnička, R. Gyepes, O. Lavastre, P.H. Dixneuf, Ferrocene-containing (η 6 -Hexamethylbenzene)ruthenium(II) methoxycarbenes: synthesis, structure, and electrochemistry, Organometallics 16 (1997) 5089–5095, https://doi.org/10.1021/om970478k.
[58] B. Therrien, L. Vieille-Petit, J. Jeanneret-Gris, P. Štěpnička, G. Süss-Fink, Ruthenium(II) complexes with ferrocene-modified arene ligands: synthesis and electrochemistry, J Organomet Chem 689 (2004) 2456–2463, https://doi.org/10.1016/j.jorganchem.2004.03.047.
[59] P. Zanello, G. Opromolla, G. Giorgi, G. Sasso, A. Togni, Redox behaviour of ferrocene derivatives VIII 1, I'-B is(diphenylphosphino) ferrocenes, 1996.
[60] J. Ludvik, P. Štěpnička, Ferrocene derivatives in voltammetric investigations of intramolecular electronic interactions, ECS Trans 2 (2007) 17–25, https://doi.org/10.1149/1.2409005.
[61] E. Sequoia, G. Pilloni, B. Longato, B. Corain, Heteropolymetallic complexes of l,l'-bis(diphenylphosphino)ferrocene (dppf) VII *. Redox behaviour of dppf, 1991.
[62] J.H.L. Ong, C. Nataro, J.A. Golen, A.L. Rheingold, Electrochemistry of late transition metal complexes containing the ligand 1,1′-bis(diisopropylphosphino) ferrocene (dippf), Organometallics 22 (2003) 5027–5032, https://doi.org/10.1021/om0340138.
[63] N.L. Weinberg, H.R. Weinberg, Electrochemical oxidation of organic compounds, Chem Rev 68 (1968) 449–523, https://doi.org/10.1021/cr60254a003.
[64] T. Sixt, M. Sieger, M.J. Krafft, D. Bubrin, J. Fiedler, W. Kaim, Ambi-valence taken literally: ruthenium vs iron oxidation in (1,1′-diphosphinoferrocene)ruthenium(II) hydride and chloride complexes as deduced from spectroelectrochemistry of the heterodimetallic "mixed-valent" intermediates, Organometallics 29 (2010) 5511–5516, https://doi.org/10.1021/om1004258.
[65] M.I. Bruce, P.J. Low, F. Hartl, P.A. Humphrey, F. De Montigny, M. Jevric, C. Lapinte, G.J. Perkins, R.L. Roberts, B.W. Skelton, A.H. White, Syntheses, structures, some reactions, and electrochemical oxidation of ferrocenylethynyl complexes of iron, ruthenium, and osmium, Organometallics 24 (2005) 5241–5255, https://doi.org/10.1021/om050483l.